AD A116786

DTIC FILE COPY

DTIC
ELECTE
JUL 12 1982
S D
D

DEPARTMENT OF PHYSICS
WASHINGTON STATE UNIVERSITY

82 07 12 022

OFFICE OF NAVAL RESEARCH
Contract N00014-80-C-0213
Project NR 092-558

Annual Technical Report
June 1982

FRACTO-EMISSION FROM POLYMERS

J. Thomas Dickinson

Department of Physics
Washington State University
Pullman, Washington 99164

SECURITY CLASSIFICATION OF THIS PAGE (When Data Entered)

REPORT DOCUMENTATION PAGE		READ INSTRUCTIONS BEFORE COMPLETING FORM
1. REPORT NUMBER	2. GOVT ACCESSION NO. AD-A[illegible]	3. RECIPIENT'S CATALOG NUMBER
4. TITLE (and Subtitle) Fracto-Emission from Polymers		5. TYPE OF REPORT & PERIOD COVERED Annual Technical Report June 1981 - June 1982 6. PERFORMING ORG. REPORT NUMBER
7. AUTHOR(s) J. Thomas Dickinson		8. CONTRACT OR GRANT NUMBER(s) N00014-80-C-0213
9. PERFORMING ORGANIZATION NAME AND ADDRESS Department of Physics Washington State University Pullman, WA 99164-2814		10. PROGRAM ELEMENT, PROJECT, TASK AREA & WORK UNIT NUMBERS NR 092-558
11. CONTROLLING OFFICE NAME AND ADDRESS Office of Naval Research Power Program Arlington, VA 22217		12. REPORT DATE June 21, 1982 13. NUMBER OF PAGES
14. MONITORING AGENCY NAME & ADDRESS(if different from Controlling Office)		15. SECURITY CLASS. (of this report) Unclassified 15a. DECLASSIFICATION/ DOWNGRADING SCHEDULE

16. DISTRIBUTION STATEMENT (of this Report)

Approved for public release; distribution unlimited

17. DISTRIBUTION STATEMENT (of the abstract entered in Block 20, if different from Report)

18. SUPPLEMENTARY NOTES

19. KEY WORDS (Continue on reverse side if necessary and identify by block number) fracture, delamination, crack propagation, fracture surfaces, surface chemistry, free radicals, interfacial failure, exo-emission, electron emission, positive ion emission, photon emission, chemi-emission, tribo-luminescence, surface charging, fracto-emission, time-of-flight mass spectroscopy, fracture of: polymers, glass, aluminum oxide, poly-butadiene, silicone rubber, PETN, HMX, elastomers, crack velocity. crack tip speed.

20. ABSTRACT (Continue on reverse side if necessary and identify by block number) Progress in the investigation of fracto-emission (FE) from polymers is reported. Measurements characterizing the FE, experiments concerning FE mechanisms, and studies of factors influencing FE are discussed. This work includes: an examination of FE accompanying adhesive failure, the crack velocity dependence of electron emission from the fracture of elastomers, experiments to measure the mass-to-charge ratio of the positive ion emission, time correlation measurements of the electron and positive ion emission, and the detection of charge particle emission from the fracture of the molecular crystals PETN and HMX.

DD FORM 1 JAN 73 1473

SECURITY CLASSIFICATION OF THIS PAGE (When Data Entered)

TABLE OF CONTENTS

I. TECHNICAL SUMMARY

Crack propagation through an insulating material or at an interface produces regions of high electronic and chemical activity at the freshly created surfaces. This activity causes the emission of particles, i.e. electrons, ions, and neutral species, as well as photons from the surfaces both during and after crack propagation. This emission is called fracto-emission, and in many ways serves as a probe of the electronic and chemical activity of the fracture surface. The work described in this report represents the results of our second year's research. Our primary goals have been to characterize fracto-emission(FE) from polymers, to further our understanding of the FE mechanisms, and the examine the dependence of FE on the fracture event and material properties. These studies have included examination of FE accompanying adhesive failure, measurements of the dependence of electron emission (EE) on crack velocity, measurements of the mass of the positive ion emission (PIE), an examination of the time correlation between the EE and PIE being emitted from the same sample, and detection of FE from the fracture of molecular crystals. Major properties and trends observed are outlined below.

1. FE is a wide-ranging phenomenon. We have observed charged particle emission from inorganic crystalline materials, ceramics, glasses, glassy polymers, filled and unfilled elastomers, fiber reinforced composites, and most recently single crystals of molecular solids.

2. The occurence of all FE components that we have observed tends to correlate with some form of crack growth and/or bond breaking. This includes small signals due to crack formation processes or larger signals accompanying dynamic crack propagation. Emission is generally most intense <u>during</u> crack growth.

3. In filled elastomers, the EE intensity grows exponentially with crack velocity, suggesting a strong dependence of the production of reactive species (which are responsible for EE) on the crack velocity.

4. The masses of the PIE which we have obtained to date appear to be produced from atomic and molecular fragments of the material fractured rather than from impurities.

5. Interfacial failure between polymers and glass, graphite, Kevlar, and metals produces very intense, long-lasting, energetic EE and PIE. This is thought to be because of the production of a high concentration of surface free radicals and a high degree of surface charge due to charge separation. Emission may last for up to two hours and have energies up to 2-3 KeV.

6. The EE and PIE time distributions tend to be identical and frequently of the same order of magnitude. For a number of systems, the EE and PIE show a substantial component in coincidence (within 0.5 μs -- due to the finite time-of-flight of the ion) suggesting that the EE and PIE share the same de-excitation process.

7. For filled polybutadiene, we have shown the existence of an excited neutral species, also emitted in coincidence with an electron.

8. The molecular crystals PETN and HMX have been shown to emit EE and PIE. This implies that fracture of such crystals involves bond breaking on a significant scale.

In Table I, we summarize the FE characteristics we study, possible mechanisms, and parameters that are known or suspected to influence FE.

TABLE I

Characteristics of FE Investigated

Types of particles emitted: electrons, ± ions, ground state neutrals, excited neutrals, photons

Species of ± ions, neutrals

Energies of electrons, ions, neutrals, photons

Time distributions relative to fracture

Possible Mechanisms Contributing to FE

Chemi-emission:

- Production of highly reactive species; e.g., free radicals displaced atoms and molecules, defects
- Production of trapped electrons
- Recombination of reactive species; annihilation of defects
- Electronic transitions during bond breaking and during recombination/defect annihilation

Charge separation yielding intense E-fields; accelerates ejected charge

Increased temperatures at the crack-tip due to crack propagation

Parameters Influencing FE

Material (e.g., composition, structure)

Sample history (e.g., exposure to radiation, temperature cycles, strain-cycles)

Temperature

External electric field

Gaseous environment

Nature of fracture (e.g., fracture mode, crack velocity, locus of fracture in multi-phase systems)

II. INTRODUCTION

The five sections that follow discuss the experimental results of fracto-emission studies we have made between June 1981-June 1982. (Note: references and figures appear at the end of each section.) Two reports were issued during this interval:

September 1981 - FRACTO-EMISSION ACCOMPANYING ADHESIVE FAILURE (published in J. Vac. Sci. and Technol. 20 436 (1982)).

November 1981 - CRACK VELOCITY DEPENDENCE OF ELECTRON EMISSION DURING FRACTURE OF FILLED ELASTOMERS (to be published in J. of Polymer Sci., Polmer Physics Edition).

The results of these two studies are summarized briefly in section III.

Sections IV - VII consist of four papers that have been recently submitted for publication:

Section IV: TIME-OF-FLIGHT MEASUREMENTS OF THE MASS-TO-CHARGE RATIO OF POSITIVE ION EMISSION ACCOMPANYING FRACTURE (Submitted to J. of Material Science).

Here we describe a method of measuring the mass-to-charge ratio of the PIE from samples where the emission occurs in bursts such as the fracture of fibers and coatings. Advantage is taken of the fact that both EE and PIE are emitted simultaneously so that one can use the EE burst as a t=0 mark for performing TOF measurements on the PIE.

Section V: TIME CORRELATIONS OF ELECTRON AND POSITIVE ION EMISSION ACCOMPANYING AND FOLLOWING FRACTURE OF A FILLED ELASTOMER (Submitted to Applied Physics Letters).

A comparison of the EE and PIE from the fracture of polybutadiene filled with small glass beads is made on time scales of seconds and sub-microseconds. Measurements of coincidence between components of EE and PIE are made showing that a mechanistic step is involved where simultaneous emission of an electron and a positive ion occurs. We also found evidence for the emission of an excited neutral species.

Section VI: MASS-TO-CHARGE RATIO AND KINETIC ENERGY OF POSITIVE ION EMISSION ACCOMPANYING FRACTURE OF A FILLED ELASTOMER (Submitted to Applied Physics Letters).

These measurements on glass-filled polybutadiene take advantage of the coincidence between EE and PIE. A time-of-flight method was devised where a start pulse is provided by the electron, and the time needed to drift through a field free space is used to determine the mass-to-charge ratio of the PIE. The results suggest molecular fragments of the polymer produced by fracture and being ejected into the vacuum.

Section VII: FRACTO-EMISSION FROM PETN AND HMX SINGLE CRYSTALS (Submitted to Applied Physics Letters).

This work describes our initial results on the fracture of molecular crystals. We have detected both EE and PIE from both materials indicating that fracture of molecular crystals can break intramolecular bonds.

In Section VIII we present a brief conclusion on the work to date.

III. SUMMARY OF PREVIOUSLY REPORTED WORK (6/81 - 6/82)

A. FRACTO-EMISSION ACCOMPANYING ADHESIVE FAILURE

In this study, measurements of EE, PIE, and photon emission (phE) from systems involving adhesive failure are presented. The systems shown include fiber-reinforced epoxy (graphite and Kevlar), polybutadiene (BR) filled with glass beads, the peeling of 3M Magic Transparent Tape from PMMA, and the delamination of 3M Filament Tape (i.e., the separation of the polyester backing from the glass filaments which adhere by a natural rubber-based adhesive).

In the case of the strands of fiber-reinforced epoxy (DOW DER 332 Bisphenol - A Type), when single fibers of the pure epoxy were fractured, bursts of EE and PIE were observed that decayed with time constants on the order of 10 - 100 μs. When the strands were fractured, the EE and PIE lasted for several minutes. We have observed such emission from Kevlar/Epoxy strands that sustained itself for as long as two hours.

Similar emission curves are seen from the fracture of glass-filled BR and the peeling and delamination of the tapes. The phE accompanying the tape experiments decayed away in a few seconds or less whereas the EE (and PIE) decayed in a very slow manner. This suggests the rate limiting steps for EE and phE are considerably different. Figures 1-4 show some of the data for BR and the adhesive tapes.

Our basic conclusions concerning FE from systems involving adhesive failure is that the intense, long-lasting EE and PIE is due to the creation of high concentrations of excited and reactive species (e.g. free radicals) during interfacial failure. The resulting exothermic reactions that occur are accompanied by non-adiabatic energy transfer processes that eject the charged particles. Our studies also indicate that the intense charge

separation that occurs during adhesive failure strongly influences the energies of the EE and PIE and possibly the emission rate. In summary, the enhanced effects we observe when interfaces are involved is likely due to a) higher concentrations of the chemical species produced by adhesive failure as opposed to cohesive failure, and b) the high degree of surface charging that occurs with interfacial failure.

B. CRACK VELOCITY DEPENDENCE OF ELECTRON EMISSION DURING FRACTURE OF FILLED ELASTOMERS.

In obtaining the data for Fig. 2 on BR filled with glass beads we noted that for a fixed filler concentration we obtained variations in the peak intensity and total counts of both the EE and PIE if the strain rate was allowed to vary; i.e., as the strain rate increased these parameters also increased. Because the average crack velocity was increasing we decided to correlate the instantaneous EE intensity and the crack velocity, V_c. To measure V_c, we used a video camera and video recorder which allowed measurement of the crack-tip position every 1/60 s. Differentiation of the resulting displacement vs time curve yielded V_c vs time. Simultaneously, the EE count rate vs time was recorded in a multichannel scalar.

These measurements were carried out for filled Silicone rubber (SI) as well as filled BR. The results from these measurements are shown in Fig. 5 and 6. Fig. 5 represents the first part of the data for $V_c < 8$ cm/sec and Fig. 6 shows the same data plus that acquired at slightly higher V_c, up to the video frame just prior to separation. The last instant of rupture occurred too rapidly (within one frame) to measure a velocity. Clearly there is a very strong, exponential-like increase of EE with V_c. Both materials showed similar behavior, differing primarily in intensity. The curves are monotonically increasing at all V_c. If the EE intensity

were simply proportional to the rate of surface area produced, then the EE count rate would be linear with V_c. We suggest that the principal cause of this strong dependence is that for more rapid detachment of the BR matrix from the glass bead surface, more primary bond scissions occur and thus lead to more reactive species formation.

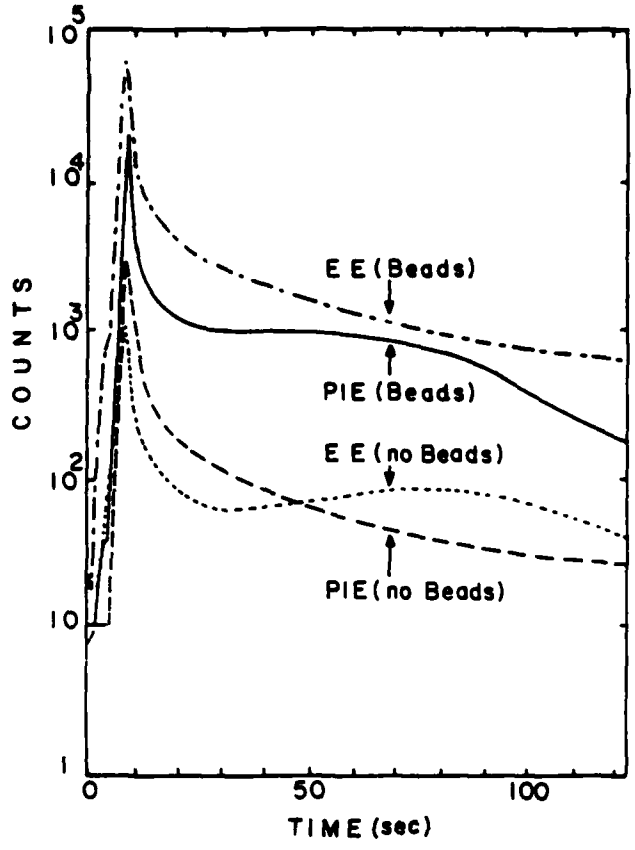

FIG. 1. EE and PIE from fracture of polybutadiene with and without glass beads.

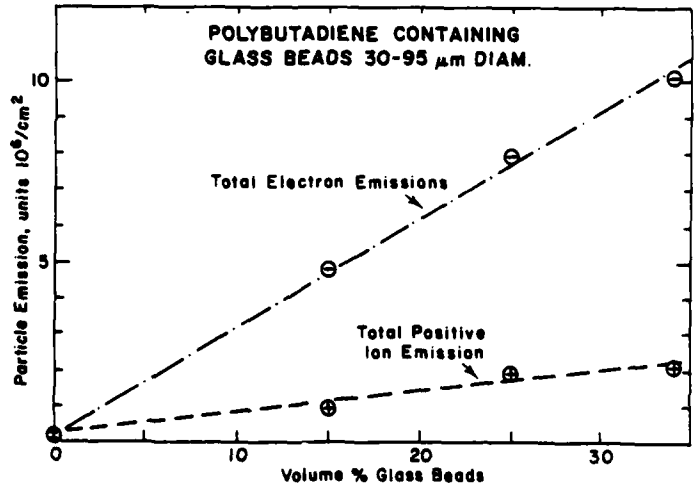

FIG. 2. The total emission (counts accumulated over 200 s) as a function of the volume percent of glass beads in polybutadiene. Polybutadiene containing glass beads 30–95 μm diam.

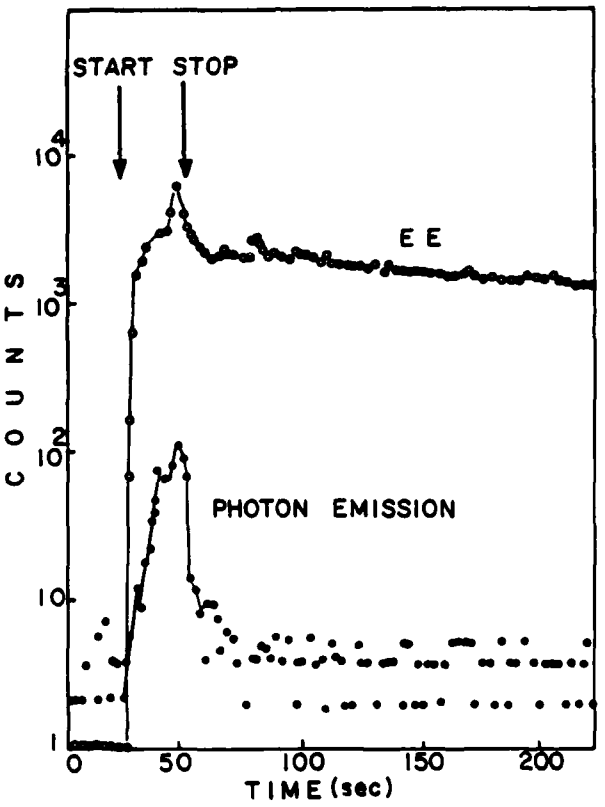

FIG. 3 EE and photons from peeling 3M-MAGIC TRANSPARENT TAPE from PMMA.

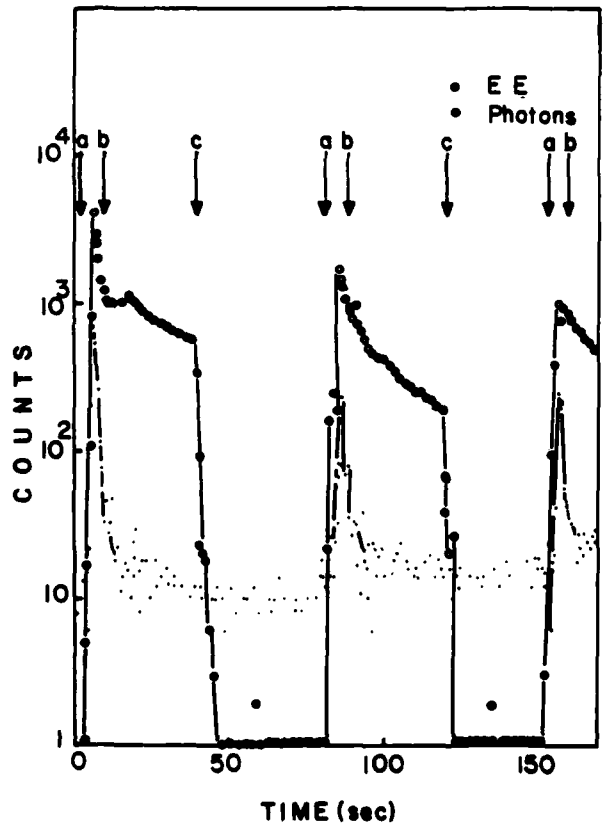

FIG. 4. EE and photons from delamination of 3M Filament Tape.

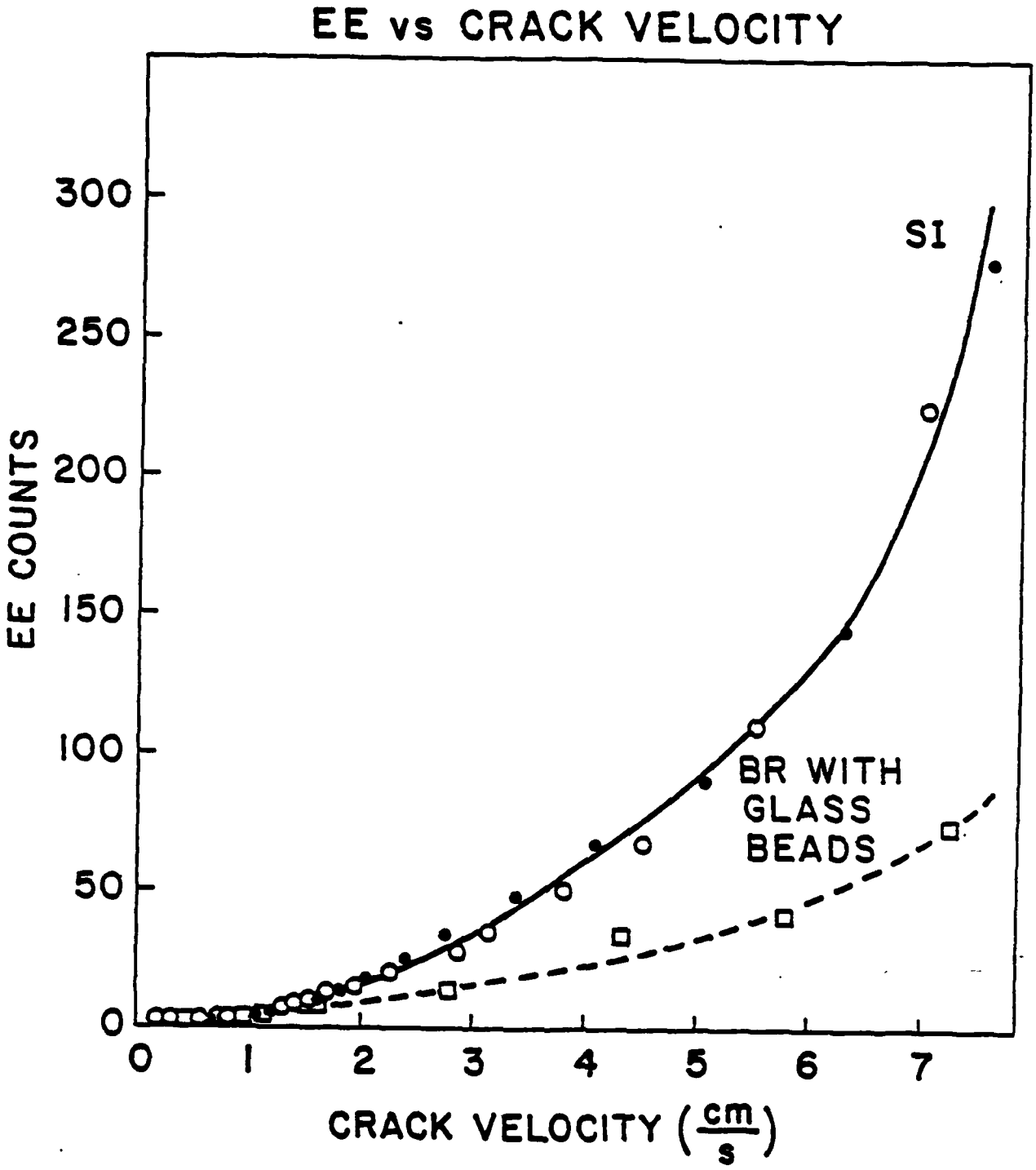

Fig. 5. Electron emission intensity vs crack velocity on a linear scale for the first part of the velocity scale. The data shown for SI are from two samples.

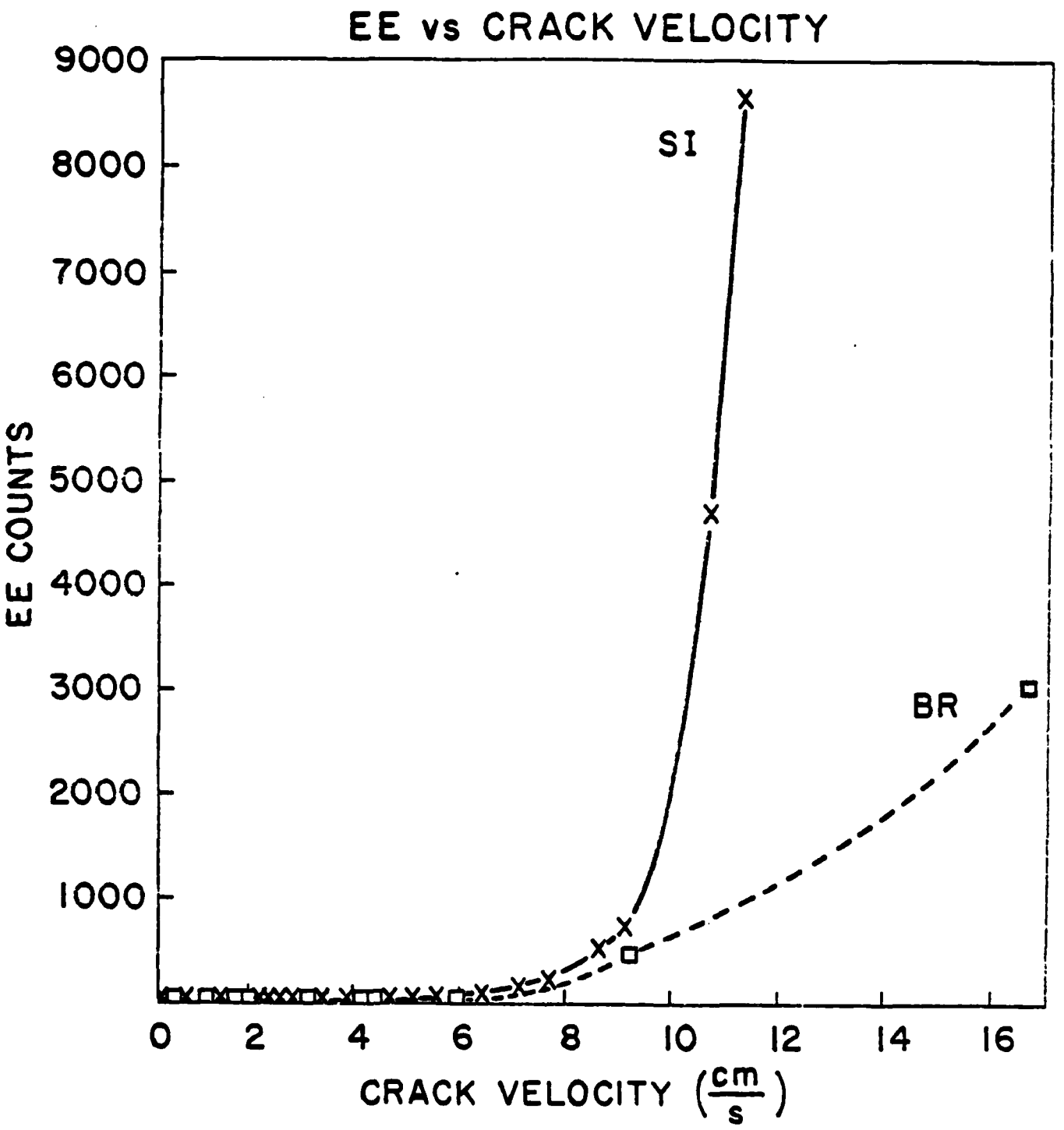

Fig. 6. Electron emission intensity vs crack velocity over the entire V_c range measured on a linear scale.

IV. TIME-OF-FLIGHT MEASUREMENTS OF THE MASS-TO-CHARGE RATIO OF POSITIVE ION EMISSION ACCOMPANYING FRACTURE

J. T. Dickinson, L. C. Jensen, and M. K. Park
Department of Physics
Washington State University
Pullman, Washington 99164-2814

ABSTRACT

When non-metals are fractured, electrons and positive ions are emitted. We report our first time-of-flight measurements of the mass-to-charge ratio (M/q) of the positive ion emission (PIE) from the fracture of Kevlar and E-glass fibers and aluminum oxide coatings. Although the uncertainty is relatively large, the M/q observed suggest that for these materials PIE is a result of molecular and atomic fragments being produced during fracture.

INTRODUCTION

A number of particle emission phenomena have been observed accompanying and following the fracture of materials. These have been collectively termed "fracto-emission" because the propagation of a crack appears to be a prerequisite for their appearance. The types of particles we and others have observed include electrons,[1-8] positive and negative ions,[1-9] neutral molecules,[10] and photons.[8,11] Positive ion emission (PIE) accompanying tensile deformation of a material was first reported by Rosenblum et al.[9] for oxide-covered metals. Dickinson et al.[3-5] showed that both PIE and electron emission (EE) from oxidized Al was due to crack propagation in the oxide coating and that the PIE and EE occurred in bursts typically less than 1 μs in duration and in coincidence with crack growth in the oxide.

In this report, we present results of a preliminary determination of the mass-to-charge ratio (M/q) of the positive ion emission (PIE) emitted from Kevlar-49[12] and E-glass fibers, and from aluminum oxide coatings. The motivation for these measurements is first to improve our understanding of the origin of PIE and second to enhance the usefulness of FE measurements for the understanding of fracture phenomena. The latter is of particular importance if the observed PIE is a product of the molecular and atomic fragments produced in crack propagation. In such a case, the ionic species observed would indicate how fracture occurred in the material. For example, in the fracture of a polymer a simple question is: during fracture, are there fragments of mass less than, equal to, or greater than the monomeric unit? PIE may also be a useful tool for examining loci of fracture in multiphase systems such as ceramics and fiber reinforced composites.

Similar questions have been raised for epoxy systems using stress-induced mass spectroscopy to monitor the neutral emission. Wolf et al.[13] have

shown that in the fracture of an epoxy resin, MY720 (Ciba-Geigy) cured with Eporal (diaminodiphenylsulfone, Ciba-Geigy) SO_2 is released which was considered part of the main chain. The uncertainties in our measurements make it difficult to give definitive answers to these questions; however, it will be shown that in the cases studied we must consider the emission of atomic/molecular fragments from fracture as strong possibilities.

EXPERIMENTAL

The polymer fibers used in this study were 10 μm Kevlar-49 aramid fibers, characterized by high crystallinity, high tensile strength and modulus, and low density. The chemical composition by weight[14] is

67% C
15.9% O
11.2% N
4.3% H
0.8% ash (including small quantities of Na and S)

The monomer unit, determined by L. Penn and F. Larsen,[14] is poly (p-phenylene terephalamide (PPD-T)):

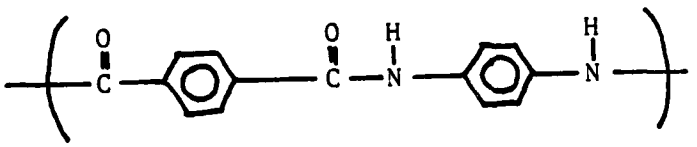

which has a mass of 162 amu. Only trace amounts of unreacted constituents and solvent are expected to be present. Due to long exposure to the atmosphere there is likely to be H_2O absorption,[14] on the order of 1-3% by weight, before introduction into the vacuum system. Although a good portion of this moisture should be removed during pump down, some H_2O certainly would remain at room temperature. Other atmospheric gases might be present, also.

The E-glass fibers were untreated and 20 μm in diameter. The chemical composition of E-glass[15] is:

53%	SiO_2
21%	CaO
15%	Al_2O_3
9%	B_2O_3
1.2%	Na_2O
.3%	MgO
.3%	BaO
.1%	K_2O

Water is the predominant absorbed molecule in glasses.[16] At elevated temperatures (above the softening temperature) constituents of the glass itself begin to break down and lead to evolution of H_2O (dehydration), CO_2, and sometimes O_2.

The fiber samples were composed of 5-20 fibers adhesively bonded to Al sheet metal shaped to fit into clamps in a vacuum system. To decrease the probability of pull-out of the fibers out of the adhesive, the fibers were stretched across a sharp Al edge, where approximately 90% of them would fracture. The fiber length was 1.5 cm. The diameters were 10 μm for Kevlar and 20 μm for E-glass. By using fibers of various lengths one could spread out in time the fracture events, although multiple breaks within a few microseconds were not uncommon when fibers were allowed to twist or cross in any way.

The aluminum oxide coatings were produced on Al 1350 substrates machined in a dog bone shape, 0.5 mm in thickness and with a gage of 10 x 30 mm. The samples were cleaned in a CrO_3 - H_2SO_4 solution and anodized in a 0.05 m ammonium tartrate solution at room temperature for 30 minutes at a voltage of 230 V. This produced a dense oxide layer of approximately 300 nm in thickness. The structure of aluminum oxides produced by anodization is known to be amorphous

in nature with varying degrees of crystallinity, depending on the electrolyte and the anodizing conditions.[17] It is also known that during the anodizing process, the anion and H_2O are incorporated to some extent into the oxide,[18-20] which tends to be hydrated. Oxygen gas is evolved at the anode which could be absorbed into the oxide layer. Thermal desorption measurements[10] on similarly grown anodized oxide films on bare Al 2024 yielded the release of O_2 and CO_2 (presumably from the tartrate anion). No evidence of N_2 or NH_3 was found. During fracture of the oxide, intense emission of neutral O_2 and CO_2 was observed.[10]

Earlier attempts to determine PIE mass using a standard quadrupole mass spectrometer (QMS) were unsuccessful due to relatively low signal-to-noise, the unknown mass, widely varying ion energy distributions, and most problematic, the transient nature of fracture. A less direct, but more practical method was developed that takes advantage of a) the rapid crack growth that occurs in thin fibers and brittle metal oxide coatings, and b) the fact that both EE and PIE are emitted "simultaneously" from the fracture surfaces. It is basically a time-of-flight (TOF) technique. Its main advantage is that the M/q values can be completely unknown and can be determined without a search.

Figure 1 shows schematically the experimental arrangement, where two channel-electron-multipliers (CEM) are positioned on two sides of the sample. The electron detector, CEM-EE, is positioned within 1 cm from the specimen and its front end is biased with +300V to attract electrons. The TOF of an electron to the CEM-EE in such an E-field is approximately 2 ns. In order to reach the PIE detector, the ions must pass from the fracture surface through a drift tube, the total flight path being 27 cm. The drift tube is biased with a voltage, -V, which determines the TOF of an ion of a given mass through the tube. The front end of the CEM-PIE is biased at -1 KV to assure efficient PIE

detection. Grids are mounted on both ends of the drift tube to prevent electric field penetration. The experiments were carried out in vacuum at a pressure of 10^{-7} torr. Details of the experimental arrangement are given in Ref. 7.

The total TOF distribution is obtained as follows: a multi-channel analyzer (MCA) set at 1 μs/channel is triggered with the first incoming electron. The PIE arriving at the CEM-PIE then produce a distribution of pulses that are accumulated in the MCA at times determined by a) their time of release from the sample and b) their TOF. If fracture produces a burst with a fast leading edge, then the fact that the sample continues to emit for several micro-seconds will not affect the leading edge of the PIE-TOF. It is this feature we use to determine M/q.

The leading edge of the PIE time distribution relative to the first electron detected was examined by removing the drift-tube and positioning the CEM-PIE within 1 cm of the sample. The leading edge of these times distributions did show a finite rise time for Kevlar. This was probably due to the fact that the Kevlar fibers were not fracturing as fast as one might expect. SEM photographs of fractured Kevlar fibers showed frequent splitting and shredding of the fibers rather than brittle fracture. This type of fracture would take longer to occur, thus leading to the finite rise time of the time distributions. For E-glass, we found that although the bursts reached a peak very rapidly (within 1 μs), the EE frequently showed emission a few microseconds before this rapid rise. This precursor was random and occurred approximately 30% of the time and is believed to be due to crack formation in the strained fiber. The result was a shift in the leading edge of the accumulated time distribution of 1 μs. These shifts in time were taken into account in the final analysis of the TOF. For the aluminum oxide coatings, the rise times of the PIE time distributions were, within our time resolution, instantaneous and therefore no correction in the TOF was used.

The total TOF, T, consists of the sum of the flight times: $t_1 + t_2 + t_3$ over the regions d_1, d_2, and d_3 shown in Fig. 1. Using Newton's second law, conservation of energy, and simple kinematics, we obtain a relation for T in terms of the ion mass-to-charge ratio M/q, the tube potential V, and the distances $d_1 = 1$ cm, $d_2 = 25$ cm, and $d_3 = 1$ cm. With substitution of these lengths the relation reduces to:

$$T = 20.1\sqrt{\frac{M/q}{V}} \qquad (I)$$

where T is in μs. When T is measured for various values of V, M/q can be determined from the slope of plots of T vs $\frac{1}{\sqrt{V}}$. Because the emitted ions have an energy distribution, the leading edge of the emitted bursts spreads in time. To increase precision, T was taken to be the value of time corresponding to half way up the leading edge of the time distributions (T at half maximum). A correction to V for the initial kinetic energy corresponding to this half maximum was determined for E-glass and Kevlar by measuring the value of T at half maximum for V = 0 (thus no acceleration) and calculating the corresponding energy using a value of M/q determined from Eq. 1 <u>without</u> this correction. These corrections were surprisingly small: 2 volts for E-glass and 4 volts for Kevlar. We were unable to make measurements of T for the oxide coatings below -500 volts because the presence of the metal substrate made the collection of both electrons and positive ions more difficult at lower tube voltages. Thus for the oxide coatings we have not made any corrections; we expect, however, that it would not be very significant compared to $|V| \geq 500$ volts.

RESULTS

Figures 2-4 show the leading edges of typical TOF distributions for positive ion emission from Kevlar, E-glass, and anodized Al for various drift

tube potentials. For the fibers, each curve represents the fracture of approximately 10 fibers. Five to Ten curves like these were acquired for each V and a distribution of T at half-maximum obtained. The average of these results were then plotted vs $1/\sqrt{V}$, as shown in Fig. 5. The error in T was estimated to be ± 1 μs. As mentioned previously, the Kevlar and E-glass T at half-maximum have been decreased to account for the measured shifts in the leading edge occurring in the initial time distributions. These corrections are 1.5 μs and 0.8 μs for Kevlar and E-glass, respectively. No measurable correction was found for the aluminum oxide coatings. A least squares fit to these data produced the lines shown in Fig. 5, where all curves have been forced through the origin, in compliance with Eq. I. The slopes of these lines were then used to calculate M/q. The values obtained are:

Material	M/q (amu)
Kevlar	60 ± 20
E-Glass	48 ± 12
Aluminum Oxide Coating	17 ± 6

DISCUSSION AND CONCLUSION

Although the uncertainties in these values of M/q are relatively large, we emphasize that the M/q of the PIE accompanying fracture of materials has previously been totally unknown. The technique we have employed here favors the detection of the lightest masses if more than one mass is emitted. Nevertheless, we have some sensitivity to the presence of heavier masses which should show up as a shoulder on the leading edge of the TOF distribution at longer times. Careful examination of a number of TOF distributions for all three materials showed no clear evidence of heavier masses. Therefore, our present results indicate that the PIE accompanying fracture from these materials consists of relatively light ions.

For each material our uncertainties do not allow a unique value of M to be assigned to the observed PIE and therefore there are a number of candidates for each material. For Kevlar, we can rule out absorbed H_2O^+ and ions of common background and atmospheric gases. If we assume q = 1, the PIE mass from Kevlar is considerably smaller than a monomer. Likely candidates could involve species like

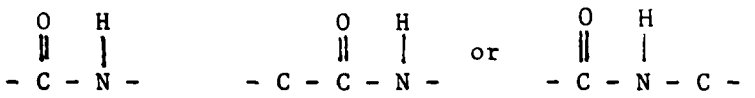

all of which would be produced by main chain bond cleavage.

For E-glass, if we assume q = 1, we can rule out H_2O^+ and O_2^+, but not CO_2^+. Fragments of the components of E-glass which are candidates include Ca^+, K^+, $B_2O_3^+$, MgO^+, and possibly SiO^+. Ohuchi et al.[21] have shown that soda-silica glass under electron bombardment (with energies between 1.5 and 10 keV) yielded emission of Na^+ via electron stimulated desorption (ESD). They estimated the bulk concentration of their samples to be 15% Na_2O and 85% SiO_2. Given the measured value of M/q in this experiment and the strong possibility that fracture induces similar intermediate states produced by ESD, we propose that we are observing Ca^+ or K^+ and note that these elements are originally bonded into the glass "lattice."

The lower M/q obtained for the aluminum oxide coating, assuming q = 1, could be one of the following: O^+, H_2O^+, OH^+, N^+, NH_x^+, or CH_x^+. All of the ions listed could be due to species entrapped in the oxide during the anodization process, although the source of O^+ or OH^+ could be from decomposition of the hydrated oxide. Again, we point out that ESD and PSD (photon stimulated desorption) studies on a number of ionically bonded, hydrated oxides[22,23] show that the predominant species desorbed during electron and soft x-ray bombardment are H^+, OH^+, and O^+. This provides support for the possibility that we are

observing either OH^+ or O^+. In either case, these would most likely be quite tightly bound in the oxide structure and either one could be considered as a product of fracture of the oxide. (One experiment that suggests itself is to study PIE from pure Al_2O_3.)

In summary, these preliminary measurements of M/q from three different materials first verify that indeed positive ions are a fracto-emission product and not an artifact induced by photon or electron emission. Second, there is a tendency for these fragments to be relatively light (10-80 amu). Third, there is a strong possibility that, for these materials, the PIE observed are fragments of the original matrix. This may be a necessity simply on the basis of energy transfer arguments: we have proposed[6-8] that PIE is intimately related to the production of high energy sites on the fracture surface by cleavage and bond breaking. These sites consist of defects in the case of oxides, displaced atoms and ions in the case of glass, and free radicals in the case of polymers. Trapped electrons available for non-radiative electronic transitions also play an important role in all these cases. The chemical reactions and electronic transitions that ensue following crack propagation then lead to ions in anti-bonding surface states, releasing the ions into the vacuum. These steps require relatively close coupling of the high energy sites and displaced atoms or molecules to be ionized and therefore, it may have to be part of or bonded to the defect structure.

In addition to furthering our understanding of PIE mechanisms, the major goals of future PIE research include: a) more precise measurements of M/q, and b) relating PIE to factors such as mode of fracture, material composition and structure, and the microscopic events occurring during fracture. The technique outlined in this paper can be used to determine approximate M/q values for a wide variety of materials. Once such values are known, as in the materials studied here, high resolution M/q measurements can be made with

little or no searching using a standard quadrupole mass spectrometer. To resolve questions concerning the source and mechanism of PIE we intend to carry out these studies on better characterized, pure materials.

ACKNOWLEDGMENTS

This work was supported in part by the Office of Naval Research, Contract N00014-80-C-0213 and by a grant from the M. J. Murdock Charitable Trust. We wish to thank R. L. Moore, Lawrence Livermore Laboratory, for providing the fiber samples.

REFERENCES

1. J. T. Dickinson, P. F. Braunlich, L. Larson, and A. Marceau, Appl. Surf. Sci. 1, 515 (1978).

2. D. L. Doering, T. Oda, J. T. Dickinson, and P. F. Braunlich, Appl. Surf. Sci. 3, 196 (1979).

3. J. T. Dickinson, D. B. Snyder, and E. E. Donaldson, J. Vac. Sci. Technol. 17, 429 (1980).

4. J. T. Dickinson, D. B. Snyder, and E. E. Donaldson, Thin Solid Films 72, 225 (1980).

5. J. T. Dickinson, E. E. Donaldson, and D. B. Snyder, J. Vac. Sci. Technol. 18, 238 (1981).

6. J. T. Dickinson and L. C. Jensen, J. Polymer Sci. Polymer Physics Ed., to be published.

7. J. T. Dickinson, E. E. Donaldson, and M. K. Park, J. Mat. Sci. 16, 2897 (1981).

8. J. T. Dickinson, M. K. Park, E. E. Donaldson, and L. C. Jensen, J. Vac. Sci. Technol., to be published.

9. B. Z. Rosenblum, P. F. Braunlich, and L. Himmel, J. Appl. Phys. 48, 5262 (1977).

10. L. A. Larson, J. T. Dickinson, P. F. Braunlich, and D. B. Snyder, J. Vac. Sci. Technol. 16,590 (1979).

11. J. I. Zink, Acc. Chem. Res. 11, 289 (1978).

12. Trade name of E. I. Dupont de Nemours and Co.

13. C. J. Wolf, D. L. Fanter, and M. A. Grayson, "Aging of Polymers and Composites," ONR Final Report MDC-Q 0743, July 21, 1981.

14. L. Penn and F. Larsen, J. Appl. Polymer Sci. 23, 59 (1979).

15. L. L. Clements, "Properties of Commercial Fibers Used for Filament-Wound Composites," Lawrence Livermore Laboratory Report UCID-17873 (1978).

16. S. Dushman and J. M. Lafferty, "Scientific Foundations of Vacuum Technique," Second Edition, John Wiley and Sons (New York, 1962), pp. 470-500.

17. J. W. Diggle, T. C. Downie, and C. W. Goulding, Chem. Rev. 69, 365 (1969).

18. J. E. Lewis and R. C. Plumb, J. Electrochem. Soc. 105, 496 (1958).

19. R. B. Mason, J. Electrochem. Soc. 102, 671 (1955).

20. R. E. Herfort, "Fundamental Investigation of Anodic Oxide Films on Aluminum Alloys as a Surface Preparation for Adhesive Bonding," U. S. Air Force Technical Report AFML-TR-76-142.

21. F. Ohuchi, M. Ogino, P. Holloway, and C. G. Pantano, Jr., Surface and Interface Analysis 2, 85 (1980).

22. M. L. Knotek, V. O. Jones, and V. Rehn, Surf. Sci. 102, 566 (1981).

23. H. Niehus and W. Losch, Surf. Sci. 111, 344 (1981).

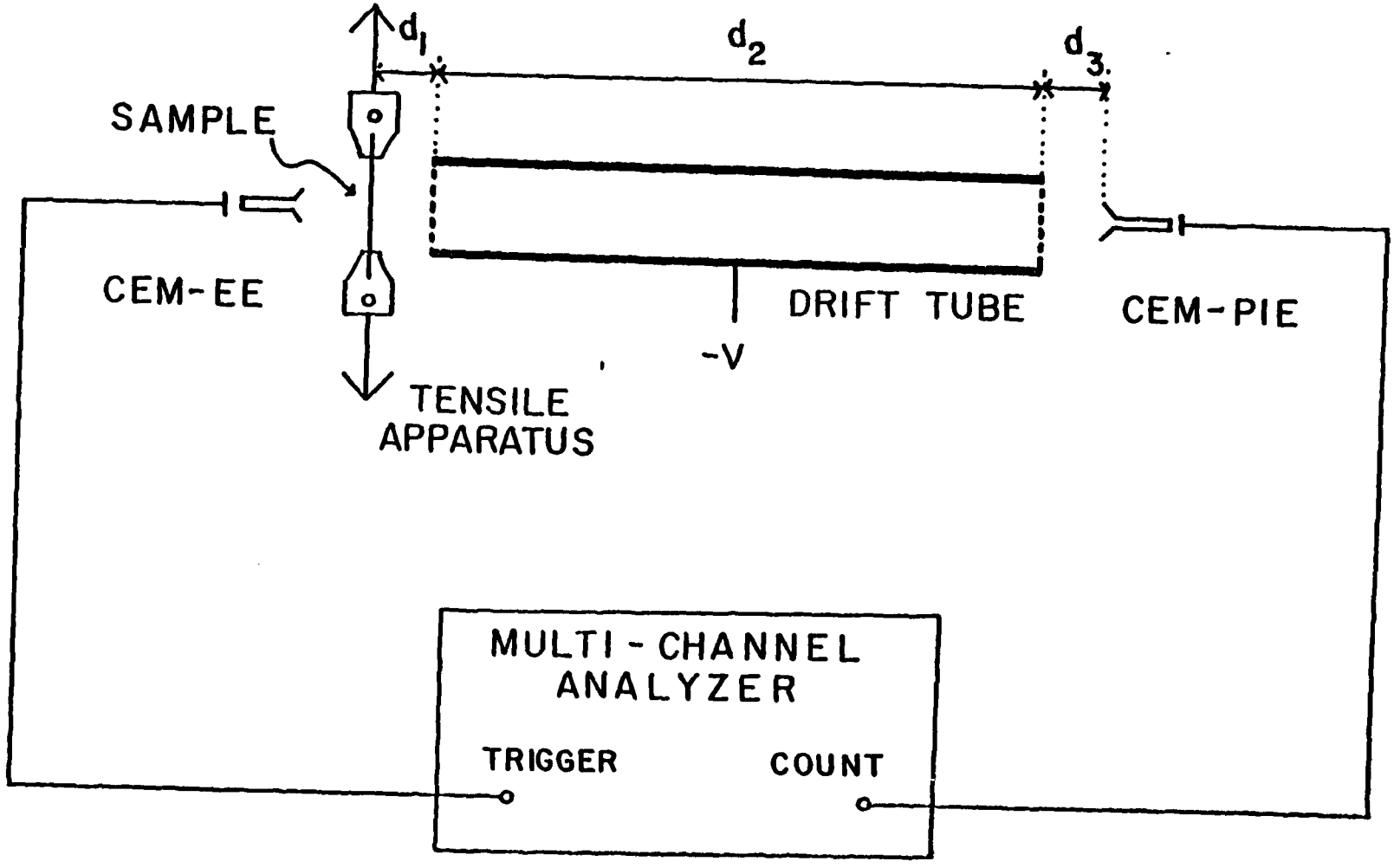

Fig. 1. Schematic of Experimental Setup. The distances are: $d_1 = d_3 = 1$ cm, $d_2 = 25$ cm.

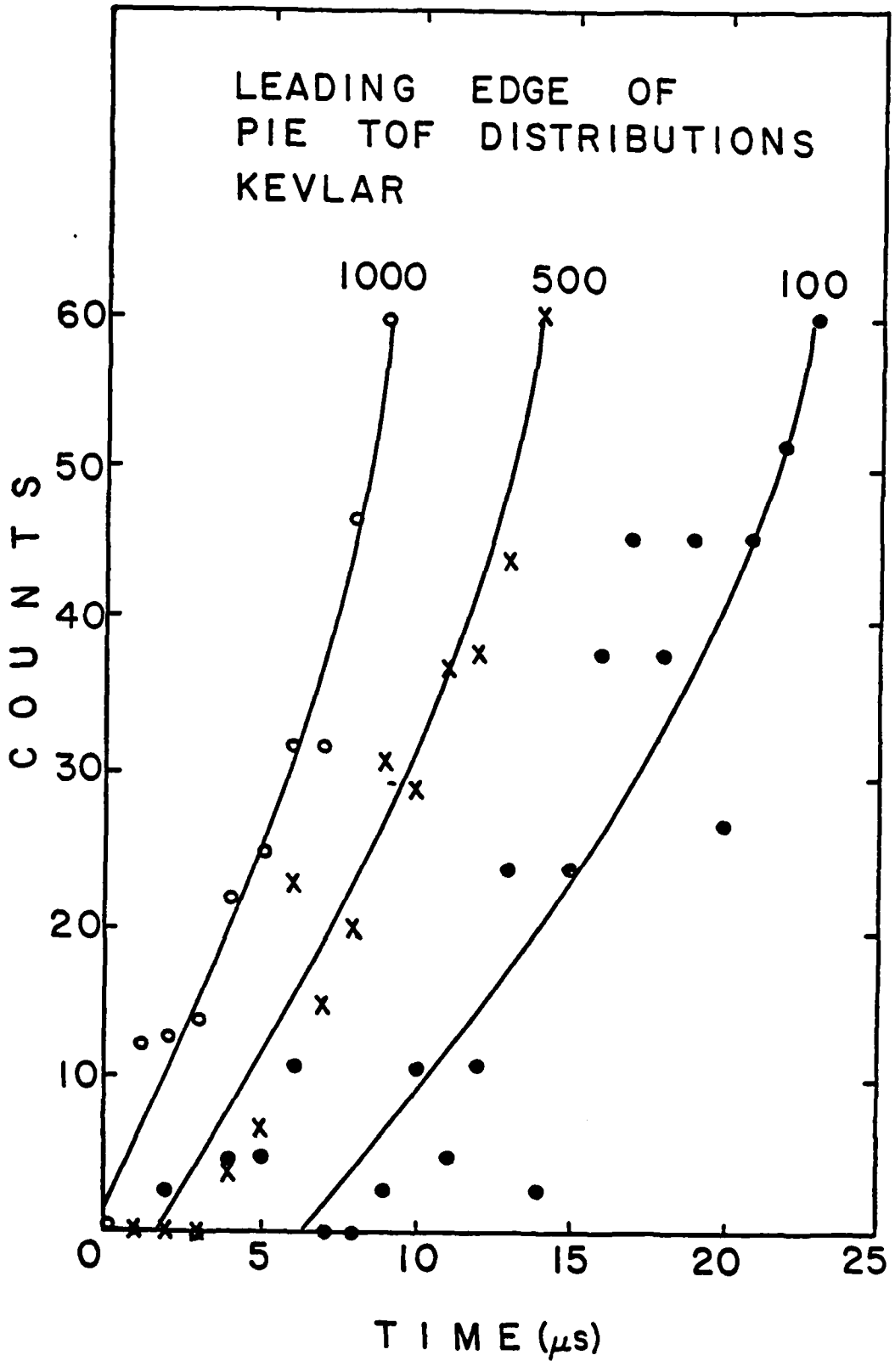

Fig. 2. Leading edge of PIE TOF distributions for Kevlar fibers.

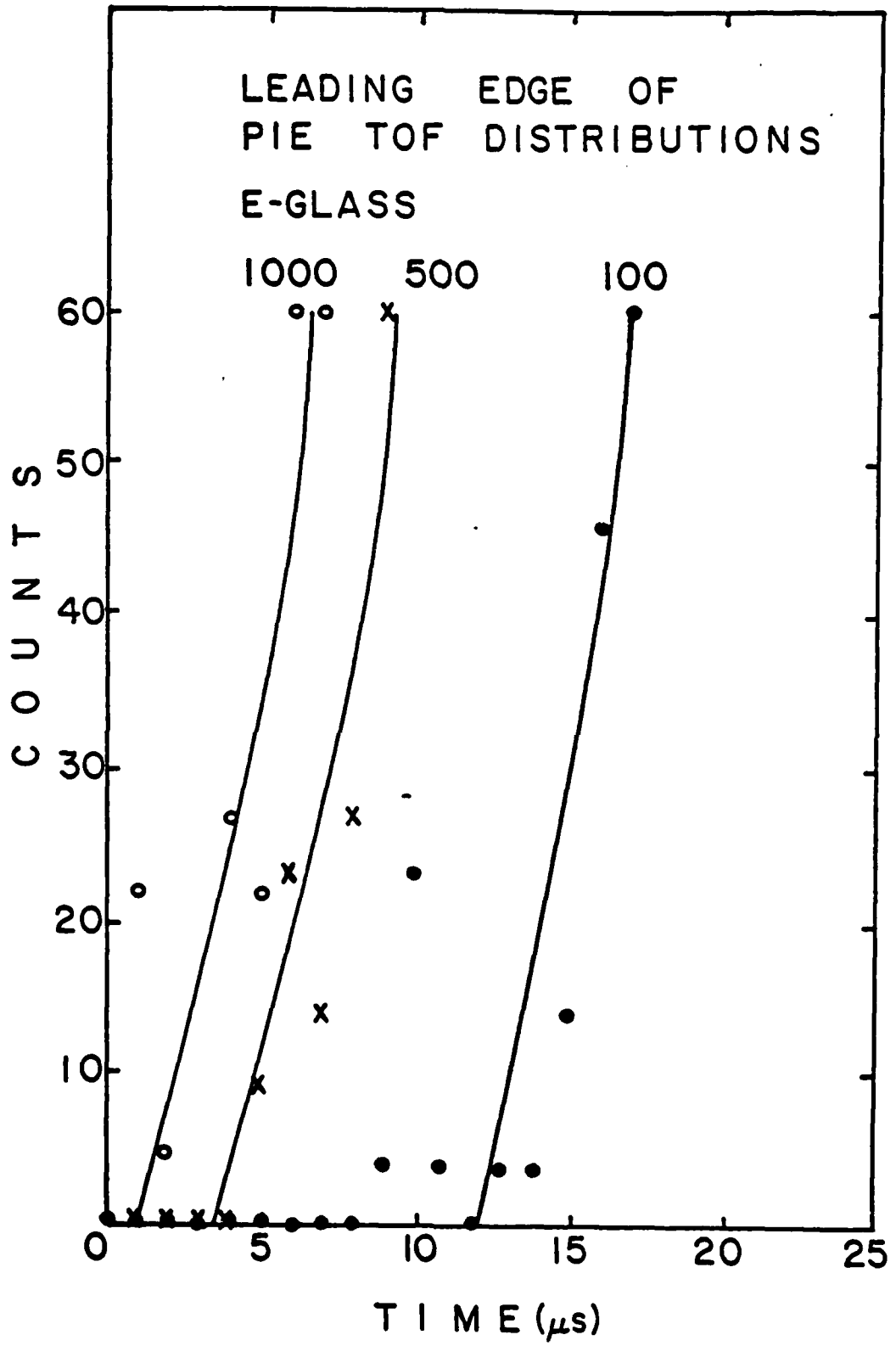

Fig. 3. Leading edge of PIE TOF distributions for E-glass fibers.

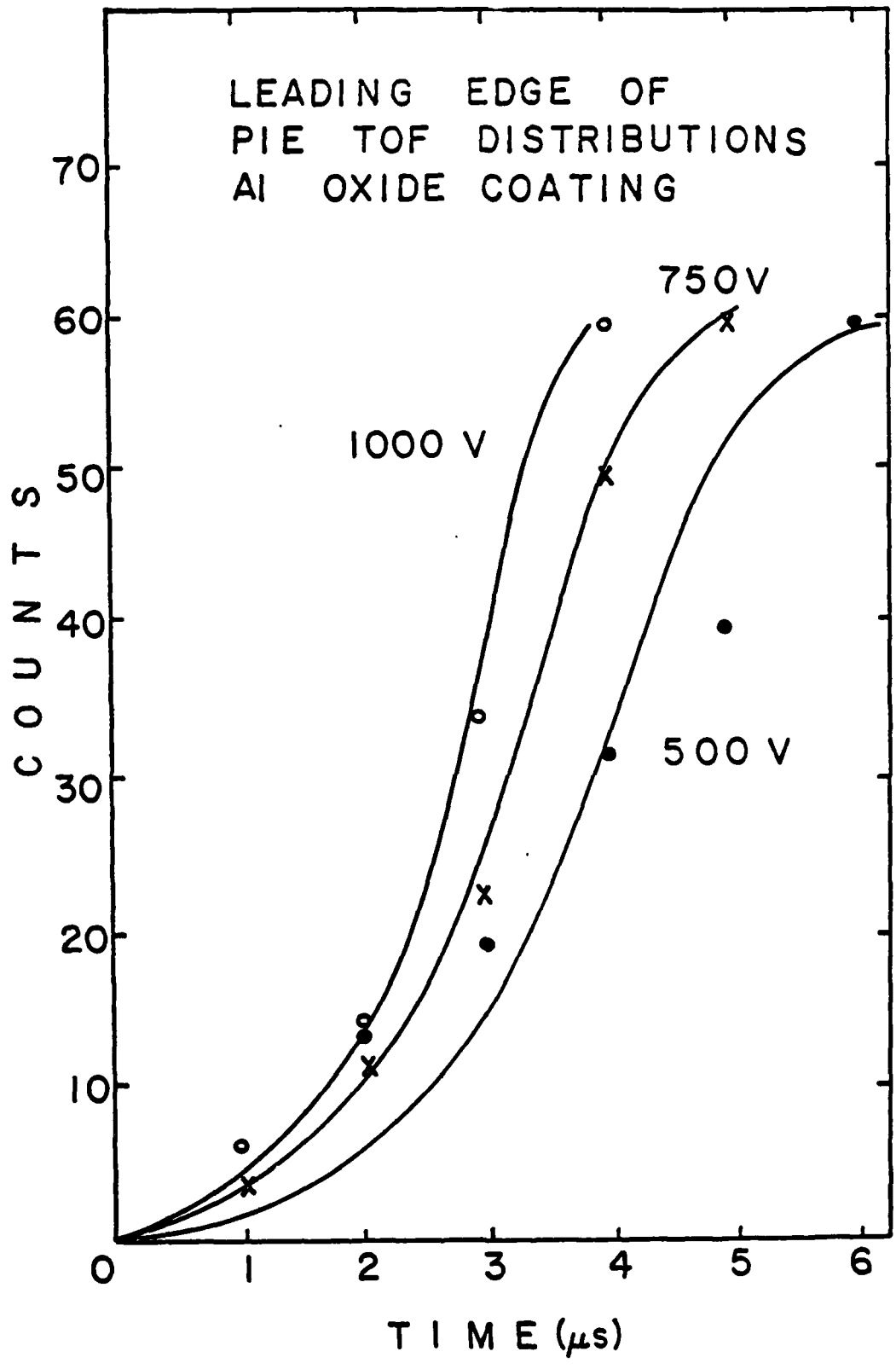

Fig. 4. Leading edge of PIE TOF distributions for Al oxide coating.

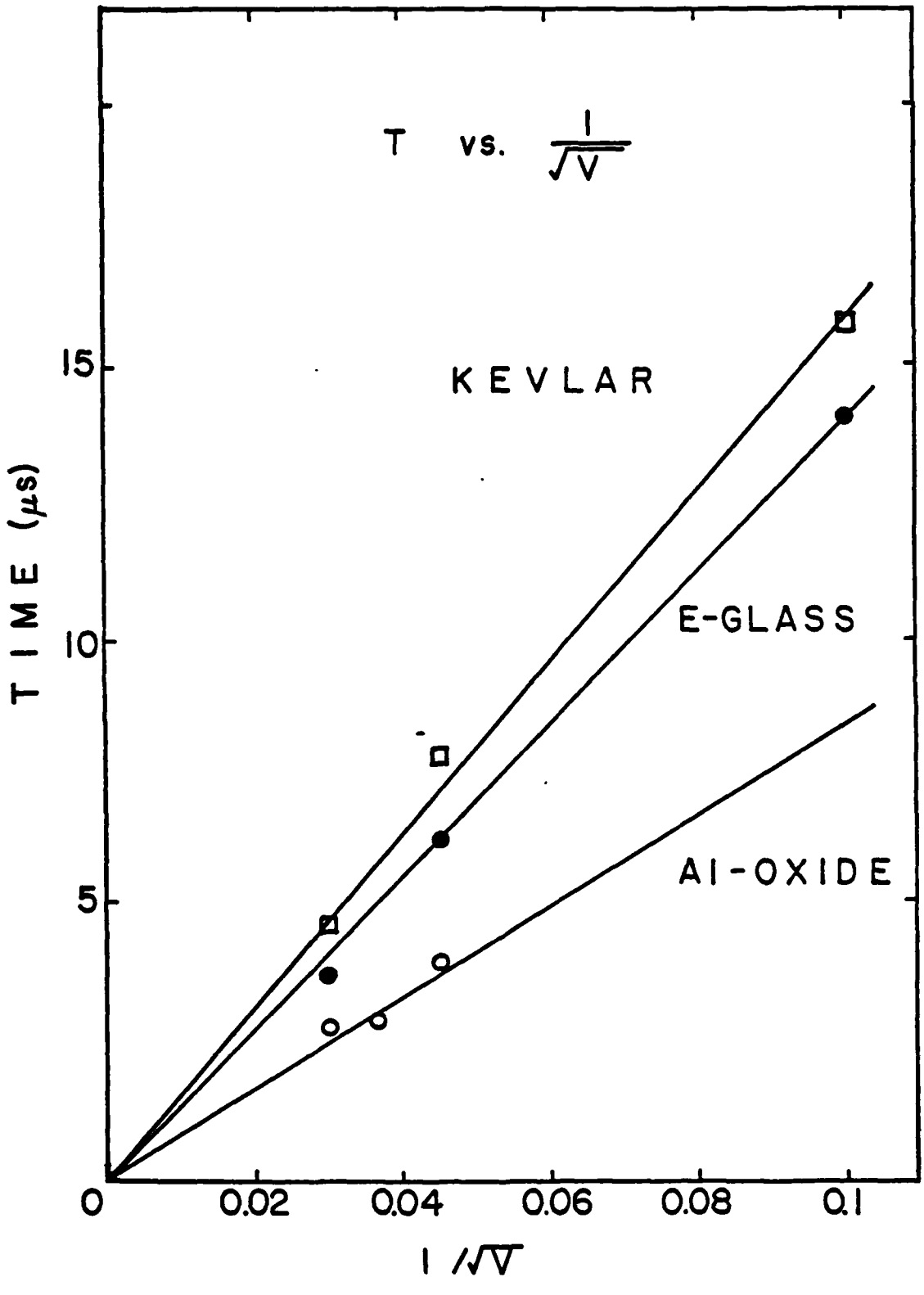

Fig. 5. Plot of T at half maximum vs $1/\sqrt{V}$(tube voltage) .

V. TIME CORRELATIONS OF ELECTRON AND POSITIVE ION EMISSION ACCOMPANYING AND FOLLOWING FRACTURE OF A FILLED ELASTOMER

J. T. Dickinson, L. C. Jensen, and M. K. Park
Department of Physics
Washington State University
Pullman, Washington 99164-2814

Abstract

When filled elastomers fracture intense electron emission (EE) and positive ion emission (PIE) accompany and follow crack propagation, two important components of what we call fracto-emission. We present here results of simultaneous measurements of EE and PIE from polybutadiene filled with glass beads. These measurements indicate: a) the EE and PIE decay kinetics are identical, b) substantial components of EE and PIE are emitted in coincidence, and c) that an excited neutral species is also emitted in coincidence with the EE.

In earlier papers[1-10] we have presented experimental results on various fracto-emission (FE) phenomena, with particular emphasis on electron emission (EE) and positive ion emission (PIE) accompanying and following the fracture of materials. For filled elastomers, we have shown the emission to be quite intense and long-lasting and that it is associated with the detachment of the elastomer from the filler particles. This interfacial or adhesive failure is believed to produce a high concentration of reactive surface species which leads to EE and PIE via chemically induced emission processes.[7-10] Analogous processes have been described as chemi-emission[11-13] on surfaces and chemi-ionization[14] in the gas phase. There are a number of potential applications[7] of FE to the study of fracture which would be greatly enhanced by better understanding of FE characteristics and mechanisms. In this letter we present results of simultaneous measurements of the EE and PIE from polybutadiene filled with glass beads. These measurements indicate that a) the EE and PIE decay kinetics are identical, b) there are substantial components of EE and PIE <u>emitted in coincidence</u>, and c) there is evidence for an excited neutral species also emitted in coincidence with the electrons. We also present results of EE-PIE coincidence measurements on several other materials where fracture involves interfacial failure.

The polybutadiene samples, provided by the Institute of Polymer Science at the University of Akron, consisted of polybutadiene (BR) containing 25% by volume untreated glass beads 30-95 μm in diameter. The rubber was cross-linked with 0.05% by weight dicumyl peroxide by heating for 2 hours at 150 C. The samples were cut with a sharp scalpel into strips 2 mm x 4 mm in cross-section adn 2.5 cm in length. These were held in clamps inside our vacuum system[7-10] and pulled in tension. The samples were notched in the center so that they would fracture in front of our detectors. The duration of crack

growth was typically 30 ms. Two Channeltron electron multipliers (Galileo Electro-Optics CEM 4039) were used for EE and PIE detectors. They each had a 10 mm front cone for efficient particle collection and were positioned on opposite sides of the sample each at a distance of 1 cm. The front cones of the two detectors were biased as follows:

CEM-EE +600V

CEM-PIE -2500V

This created an E-field which favored separation and simultaneous detection of the EE and PIE. The CEM pulses were approximately 50 ns wide.

Figure 1 shows on a log scale the EE and PIE measured simultaneously from the fracture of a BR sample filled with glass beads, showing the rapidly rising curves that fall in a fashion we have previously described.[7-10] The EE has been normalized to the PIE to show that over the entire time interval, the EE and PIE are following identical decay kinetics.

By connecting the EE and PIE pulses to the inputs of a coincidence circuit (Harshaw NL-20) with a 0.5 μs window we could determine if any of the electrons and positive ions were emitted in coincidence. Calculations of the time-of-flight (TOF) of a singly charged ion with zero initial kinetic energy in the E-fields indicated that an ion of mass $\leq$ 300 amu, emitted in perfect coincidence, would be detected in coincidence. Figure 2 shows typical results where we plot both the PIE vs time and the EE-PIE coincidence count rates vs time. Although not shown, the EE counts were taken simultaneously, and followed the PIE curve. From the standard equation for accidental coincidence count rate, $\dot{n}_A$,

$$\dot{n}_A = \dot{n}_{EE}\,\dot{n}_{PIE}\,\Delta t$$

where $\dot{n}_{EE}$ and $\dot{n}_{PIE}$ are the EE and PIE count rates and Δt is the

coincidence circuit time window (0.5 μs). We calculated $\dot{n}_A$ for each time and subtracted it from the measured values to form $\dot{n}_C$, the true coincidence rate. At the peak emission rate, $\dot{n}_A$ was 22000 counts/sec and $\dot{n}_C$ was 3000 cps; at 400 seconds $\dot{n}_A$ was 0.06 counts/sec and $\dot{n}_C$ was 2.5. In Fig. 2 we have normalized $\dot{n}_C$ by a constant multiple to display the similarities between $\dot{n}_C$ and $\dot{n}_{PIE}$. The ratio of $\dot{n}_C$ to $\dot{n}_{PIE}$ was observed to remain constant (in this experiment $\dot{n}_C/\dot{n}_{PIE} = 0.14$) for as long as 2 hours after fracture. At low count rates, the coincidences can be seen to occur as single counts, suggesting that a single ion and single electron are being emitted.

This ratio, $\dot{n}_C/\dot{n}_{PIE}$, was found to depend critically on the bias voltages placed on the CEM cones and on the positioning of the CEMs relative to the fracture surface, increasing this ratio when collection of emission normal to the fracture surface was expected to be enhanced. The largest ratio we measured was 0.5.

To further characterize the time-relation of the PIE relative to the accompanying electron, we measured the time delay spectrum of the positive ion relative (in time) to the detected electron, using a Nuclear Data TOF module with a time resolution of 1/4 μs/channel. The resulting time delay spectrum plotted on a log scale is shown in the upper curve of Fig. 3, where a cone voltage of -2500V was used. There are two features, the first maximum occurs in the first channel (0 to 0.25 μs); and another maximum at 1.5 μs.

The shape of the first peak exhibits a narrow but measurable half width of approximately 0.3 μs. Preliminary results from measurements of the PIE mass and initial kinetic energy using TOF techniques, which will soon be submitted for publication, show that the largest PIE mass from glass-filled BR is 230 amu. If we assume 0 eV as an initial kinetic energy, calculations show a maximum TOF to the CEM-PIE of 0.4 μs. Thus, the tail of this distribution

appears to be accounted for by the ion TOF so that the actual time difference between ion and electron ejection is estimated to be less than or equal to 0.25 μs.

The second peak at 1.5 μs was at first thought to be a massive ion, again accompanying EE. However, changing the voltage on the cone of the CEM-PIE had no effect on its position. The resulting time delay spectrum taken with the cone biased at -200V (which reduces the ion collection and detection efficiencies) is shown in the lower curve in Fig. 3. The 1.5 μs peak is clearly unshifted whereas the first peak has actually shifted into the second channel due to the longer TOF. We therefore conclude that the unshifted 1.5 μs peak is due to an excited neutral species, emitted in coincidence with the electron, with a life-time sufficiently long to survive the 1-2 μs flight time to the CEM-PIE.

With detectors in fixed positions, and fixed cone voltages normal to the samples, a number of other polymeric systems involving interfaces have been tested for EE-PIE coincidence. These all showed clear components in coincidence with the $\dot{n}_C/\dot{n}_{PIE}$ values shown in Table I for $\Delta t = 0.5$ μs.

TABLE I

Materials Showing EE-PIE Coincidence

Material	True Coincidence Rate / Positive Ion Count Rate
Polybutadiene filled with glass-beads	0.14
Styrene-Butadiene Co-Polymer filled with glass beads	0.04
Red Silicone Rubber	0.05
Solithane filled with glass-beads	0.05
Filled Vinyl Rubber	0.22
E-glass/Epoxy Composite Strand	0.02
Kevlar/Epoxy Composite Strand	0.03

In addition, we tested one unfilled polymer, namely polybutadiene, which showed a $\dot{n}_C/\dot{n}_{PIE}$ value of 0.06. Thus the occurrence of EE-PIE coincidence is not restricted to systems involving interfacial failure. These ratios, as previously mentioned, are critically dependent on the escape, collection, and detection probabilities of the two particles. For high initial kinetic energy and ejection normal to the fracture surface, the collection probabilities will be reduced. Our energy distribution measurements[7,9] on EE and PIE and those of Deryagin et al.[15] on EE accompanying adhesive failure show large high energy components. Klyuev et al.[16] have also investigated the angular distributions of EE accompanying adhesive failure and found it to be strongly peaked in the direction of the normal. Thus, the actual probability of simultaneous electron and positive ion emission is expected to be considerably higher than these measured values.

The occurrence of this strong EE-PIE coincidence component both during fracture and over long time periods afterwards and the fact that EE, PIE, and the EE-PIE COINCIDENCE curves are all identical in shape suggests that the mechanism involving these coincidence components is the dominant EE and PIE mechanism. In terms of a reaction-induced excitation, the following steps would be expected to occur:

(I) $(A + B) \rightarrow (A + B)^*$ Reaction-Induced Excitation

(II) $(A + B)^* \rightarrow C^+(v) + e^-(v)$ De-excitation

where A and B represent the displaced species produced by fracture, $(A + B)^*$ represents an excited intermediate, and $C^+(v)$ and $e^-(v)$ represent the ions and electrons ejected into the vacuum. A possible intermediate that would lead to the simultaneous appearance of $C^+(v)$ and $e^-(v)$ is an auto-ionization state. Another possibility is that ionization is a multi-electron process that involves Auger transitions that lead to the accompanying electron being ejected.

Furthermore, we suggest that the 1.5 μs peak in Fig. 3, attributed to one or more excited neutral species, may be due to the reneutralization of the departing ions; i.e.,

$$\text{(III)} \qquad C^+(\text{departing from the surface}) + e^-(\text{surface}) \rightarrow C^*(v)$$

where $C^*(v)$ is the neutralized C^+ in an excited state, ejected into the vacuum. This process can occur with high efficiency in the first few angstroms above the surface via adiabatic resonance and Auger-type transitions described by Hagstrum[17] and is believed to have been observed in electron-stimulated desorption (ESD),[18] the sputtering process,[19] and ion scattering.[20] Optical radiation from ESD of excited neutral particles has also been observed,[21] although the mechanisms are still uncertain.

We are currently attempting TOF measurements over an extended drift space on the ion and neutral components to determine the ion masses and energies, the energy-to-mass ratios of the excited neutral species, and perhaps the $C^*(v)$ life-time.

We wish to thank Dr. A. N. Gent, University of Akron Institute of Polymer Science for providing us with a number of the elastomer samples and R. L. Moore, Lawrence Livermore Laboratory, for providing the fiber/epoxy strands. We also thank E. E. Donaldson for helpful discussions.

This work was supported by the Office of Naval Research, Contract N0014-80-C-0213 and by a grant from the M. J. Murdock Charitable Trust.

References

1. J. T. Dickinson, P. F. Braunlich, L. Larson, and A. Marceau, Appl. Surf. Sci. 1, 515 (1978).

2. D. L. Doering, T. Oda, J. T. Dickinson, and P. F. Braunlich, Appl. Surf. Sci. 3, 196 (1979).

3. L. A. Larson, J. T. Dickinson, P. F. Braunlich, and D. B. Snyder, J. Vac. Sci. Technol. 16, 590 (1979).

4. J. T. Dickinson, D. B. Snyder, and E. E. Donaldson, J. Vac. Sci. Technol. 17, 429 (1980).

5. J. T. Dickinson, D. B. Snyder, and E. E. Donaldson, Thin Solid Films 72, 225 (1980).

6. J. T. Dickinson, E. E. Donaldson, and D. B. Snyder, J. Vac. Sci. Technol. 18, 238 (1981).

7. J. T. Dickinson, E. E. Donaldson, and M. K. Park, J. Mat. Sci. 16, 2897 (1981).

8. J. T. Dickinson and L. C. Jensen, J. Polymer Sci. Polymer Physics Ed., in press.

9. J. T. Dickinson, M. K. Park, E. E. Donaldson, and L. C. Jensen, J. Vac. Sci. Technol., in press.

10. J. T. Dickinson, L. C. Jensen, and M. K. Park, J. Mat. Sci., in press.

11. I. V. Krylova, Uspekhi Khimii 45, 2139 (1976).

12. J. Harris, B. Kasemo, and E. Tornqvist, Chem. Phys. Letters 52, 538 (1977).

13. B. Kasemo, E. Tronqvist, J. K. N. Øorkov, and B. I. Lundqvist, Surf. Sci. 89, 554 (1979).

14. M. S. Munson and F. H. Field, J. Am. Chem. Soc. 88, 2621 (1966).

15. B. V. Deryagin, N. A. Krotova, and V. P. Smilya, Adhesion of Solids, English Translation (Consultants Bureau, New York, 1978).

16. V. A. Klyuev, V. I. Anisimova, Yu. P. Toporov, N. A. Krotova, and B. V. Deryagin, Kolloidnyi Zhurnal 40, 244 (1978).

17. H. D. Hagstrum, in Inelastic Ion-Surface Collisions, edited by N. H. Tolk, J. C. Tully, W. Heiland, and C. W. White (Academic Press, New Yrok, 1977), p. 1.

18. I. G. Newsham and D. R. Sandstrom, J. Vac. Sci. Technol. 10, 39 (1973).

19. P. Williams, Surf. Sci. 90, 588 (1979).

20. W. Heiland and E. Taglauer, in Inelastic Ion-Surface Collisions, edited by N. H. Tolk, J. C. Tully, W. Heiland, and C. W. White (Academic Press, New York, 1977), p. 27.

21. N. H. Tolk, L. C. Feldman, J. S. Kraus, R. J. Morris, M. M. Traum, and J. C. Tully, Phys. Rev. Letters 46, 134 (1981).

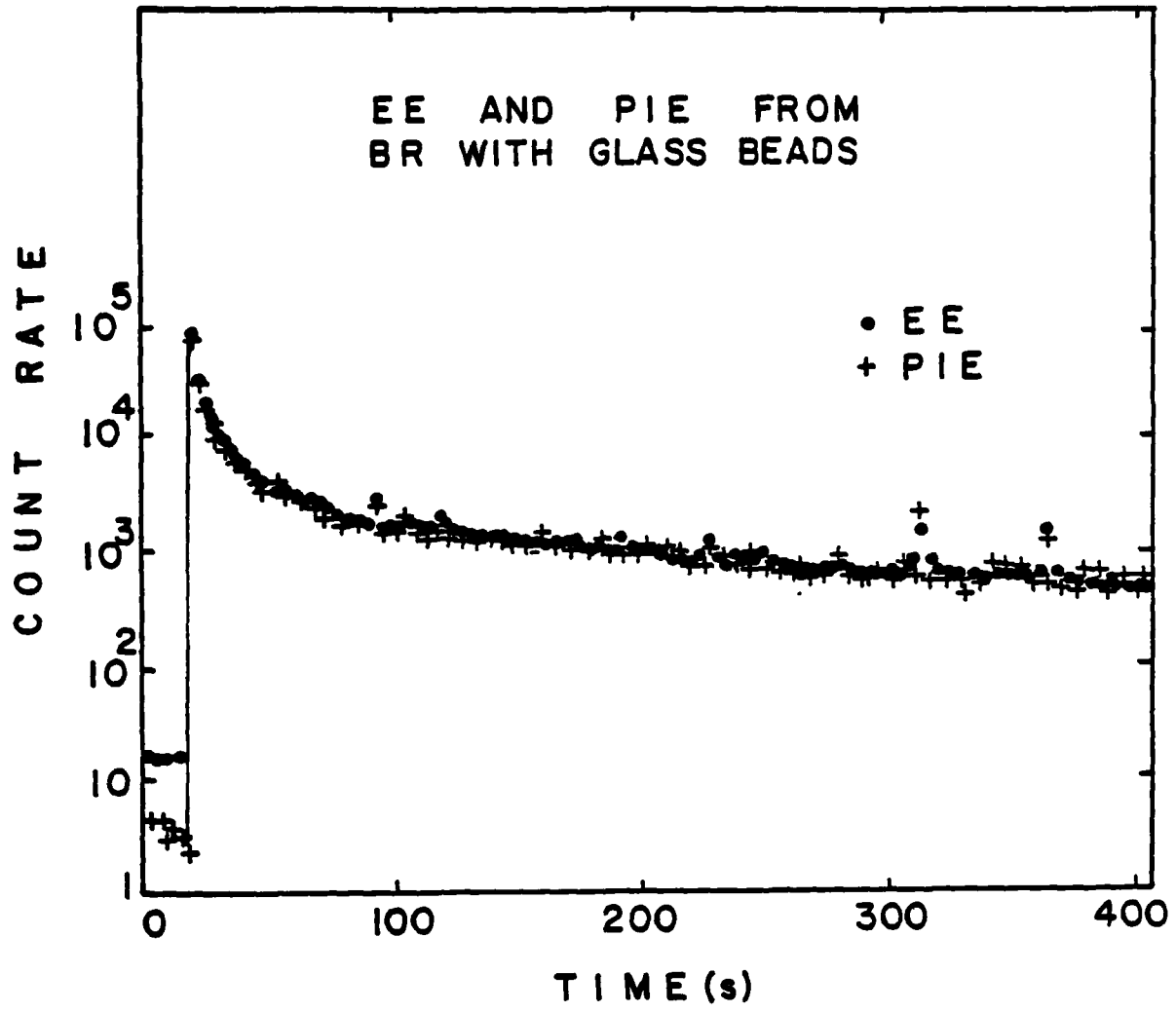

Fig. 1. The electron and positive ion emission accompanying and following fracture of polybutadiene filled with small glass beads. The EE has been normalized to the PIE to show the similarity in decay kinetics.

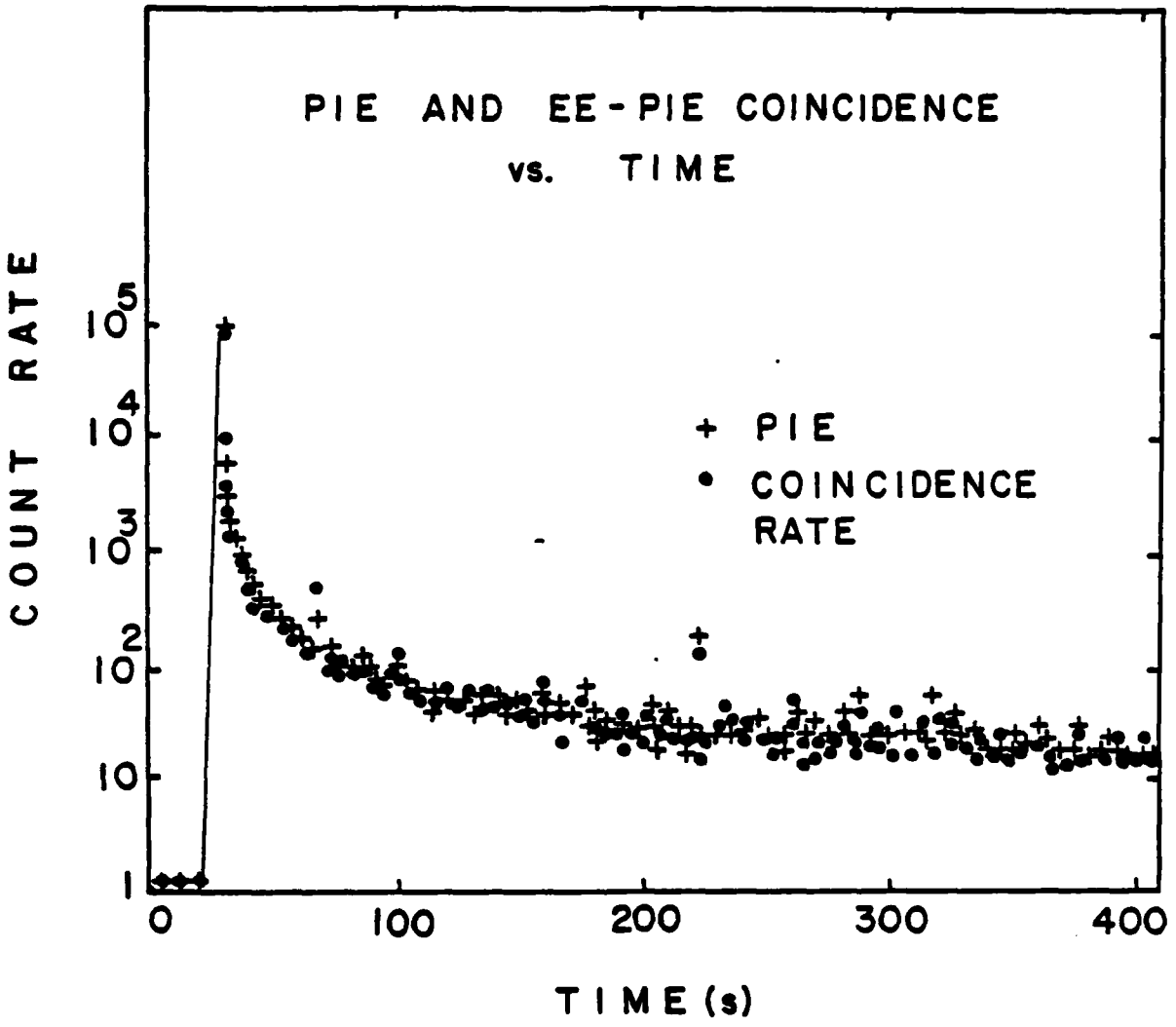

Fig. 2. The positive ion emission and the true EE-PIE coincidence count rate, $\dot{n}_C$ (corrected for accidental coincidences), accompanying and following the fracture of polybutadiene filled with small glass beads. $\dot{n}_C$ has been normalized to the PIE to show the similarities in shape.

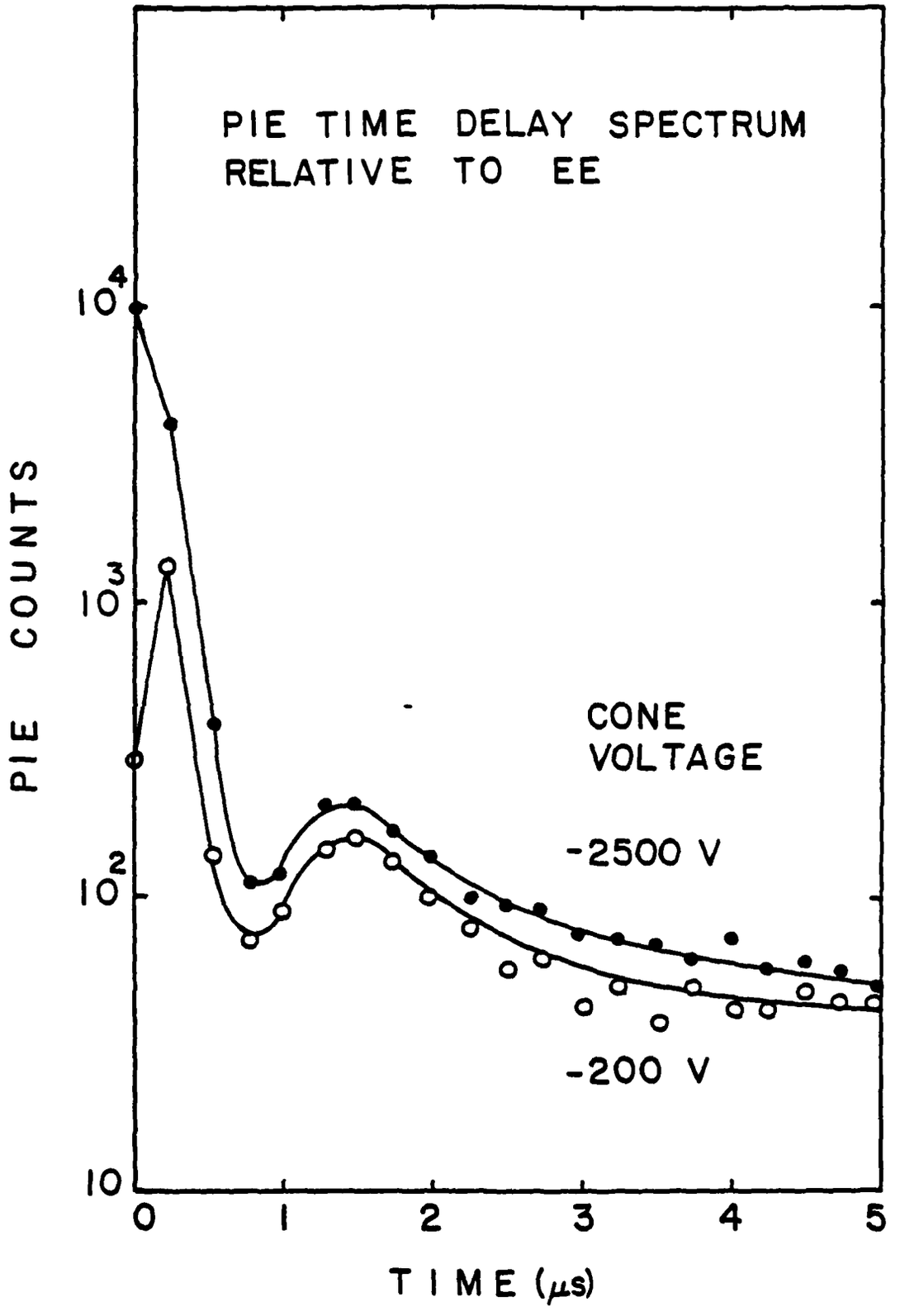

Fig. 3. The time delay spectrum of the particles detected at the CEM-PIE relative to the electrons detected at the CEM-EE. The two curves are for two voltages applied to the front cone of the CEM-PIE. The peak at 1.5 μs did not shift with this voltage.

VI. MASS-TO-CHARGE RATIO AND KINETIC ENERGY OF POSITIVE ION EMISSION ACCOMPANYING FRACTURE OF A FILLED ELASTOMER

J. T. Dickinson, L. C. Jensen, and M. K. Park

Department of Physics
Washington State University
Pullman, Washington 99164-2814

ABSTRACT

We have recently discovered that the electron emission (EE) and positive ion emission (PIE) accompanying and following fracture of filled elastomers have substantial components emitted in coincidence. We exploit this result by using a time-of-flight method to measure the mass-to-charge ratio and kinetic energy of the PIE from the fracture of polybutadiene filled with glass beads.

When non-metals are fractured, a number of particles including electrons, ions, neutral species, and photons (collectively known as fracto-emission (FE)) are emitted.[1-10] Systems that undergo interfacial or adhesive failure during fracture have been found to produce very long lasting electron emission (EE) and positive ion emission (PIE). We have recently shown[11] that for a number of systems the EE and PIE have substantial components that occur in coincidence to within 0.2 μs or less. In this letter we present measurements that exploit this coincidence to determine the mass-to-charge ratio (M/q and initial kinetic energy of the PIE components in coincidence with the EE.

The method employs a time-of-flight (TOF) technique. Figure 1 is a schematic diagram of the experimental arrangement. Two channel-electron multipliers (CEM), Galileo Electro-Optics CEM 4039, are positioned as shown. The electron detector, CEM-EE, is positioned 1 cm from the specimen and its front end is biased with $+V_{EE}$ = 600 volts to attract electrons and repel ions. The TOF of an electron to the CEM-EE is approximately 1-2 ns. For the PIE to reach the positive ion detector, CEM-PIE, the ions must pass from the fracture surface through a drift tube biased at a voltage, -V, which determines the TOF of an ion of a given M/q through the tube. The front end of the CEM-PIE is biased at a negative voltage, -2.5 kV, for efficient detection of the positive ions exiting the drift tube. Grids are mounted at both ends of the drift-tube to reduce electric field penetration. The distances shown in Fig. 1 are d_1 = 1 cm, d_2 = 25 cm, and d_3 = 1 cm. The experiments were carried out in vacuum at a pressure of 1×10^{-7} Torr in a system evacuated with a liquid nitrogen trapped diffusion pump.

The polybutadiene samples, provided by the Institute of Polymer Science at the University of Akron, consisted of polybutadiene (BR) containing 25%

by volume untreated glass beads 30-95 μm in diameter. The rubber was cross-linked with 0.05% by weight dicumyl peroxide by heating for 2 hours at 150 C. The samples were cut with a sharp scalpel into strips 2 mm x 4 mm in cross-section and 2.5 cm in length. The samples were held in small clamps and pulled in tension. The samples were notched in the center so that they would fracture in front of the CEM-EE and entrance to the drift-tube. The duration of crack growth was typically 30 ms.

During and after fracture a TOF distribution was acquired by use of a specially equipped multichannel scaler (MCS) such that the channel number was proportional to the PIE flight-time relative to the EE start pulse. The time resolution was 0.25 μs/channel. After many repetitions of triggering the MCS with the electrons, a TOF distribution was built up in the analyzer memory. This was done for several samples with various values of drift tube voltage (-V).

Figure 2 shows a TOF distribution obtained from the fracture of a single sample for a tube voltage of 2000 V. Note that there are four peaks, all being very reproducible for the several samples tested, indicating four distinct values of M/q. Studying the positions of these peaks as a function of V yielded the data shown in Fig. 3, where we have plotted the TOF peak positions vs $1/\sqrt{V}$, each curve corresponding to one of the peaks in Fig. 2. If the TOF was given simply by:

$$t_2 = \frac{d_2}{v} = \frac{d_2}{\sqrt{\frac{2qV}{M}}} \qquad \text{(I)}$$

where t_2 is the time in the drift-tube

v = drift velocity

d_2 = length of drift-tube

q = positive ion charge

M = positive ion mass

V = voltage on drift-tube

then these curves in Fig. 3 should be straight lines passing through the origin. They are not, primarily because the PIE has an initial kinetic energy, E_o, so that V in Eq. (I) must be replaced by $B' = V + \frac{E_o}{q}$.

We have examined the effect on the curves in Fig. 3 of introducing various energy distributions, n(E) for each M/q component, consistent with the shapes of the TOF spectra and have found that a unique value of an average initial kinetic energy, $\bar{E}_o$ produces the desired behavior. In Fig. 4 we show the resulting corrected TOF vs $1/\sqrt{V'}$ where we have also subtracted off small calculated corrections for t_1, the time it takes an ion to enter the drift-tube, and t_3, the time from exiting the drift-tube until the particle strikes the detector. The equations for these times are:

$$t_1 = \sqrt{\frac{2M\bar{E}_o d_1^2}{q^2V^2}} \cdot \left[\sqrt{1 + \frac{qV}{E_o}} - 1\right] \qquad \text{(II)}$$

$$t_3 = \frac{d_3\sqrt{2M\ (E_o + qV)}}{q[V_{PIE} - V]} \cdot \left(\sqrt{1 + \frac{q(V_{PIE} - V)}{\bar{E}_o + qV}} - 1\right) \qquad \text{(III)}$$

where d_1 and d_3 are the distances defined in Fig. 1

V_{PIE} = the magnitude of the voltage on the front cone of the CEM-PIE

$\bar{E}_o$ is the average initial kinetic energy of the positive ion.

These corrections, t_1 and t_3, add up to approximately 5% of t_2. By using an iterative process of adjusting $\bar{E}_o$ and M, the four curves of Fig. 3 quickly converge to the four curves shown in Fig. 4. The fact that $\bar{E}_o$ came out the <u>same</u> for each M/q was somewhat surprising. The value obtained was $\bar{E}_o$ = 1300 eV with a width of no more than ± 100 eV.

The M/q values corresponding to the four curves in Fig. 4 are given in Table I.

TABLE I

Curve	M/q amu/e	Possible Fragments			
		From BR Alone		From BR + Oxygen	
A	85 ± 6	H H B-C-C H	(81)	B-O-O	(86)
B	123 ± 6	H B-B-C H	(122)	B-B-O	(124)
C	170 ± 6	H B-B-B-C H	(176)	O-O-B-B-O-O	(172)
D	230 ± 6	H B-B-B-B-C H	(230)	B-B-B-B-O	(232)

In considering the source of such M/q values we cannot absolutely rule out extrinsic species such as background gases and impurities in the polymer. We are still in the process of determining the possible role of contaminants from the gaseous background. However, one test performed in a UHV system at a pressure of 10^{-8} Torr[7] involved the detection of PIE from the fracture of an E-glass/epoxy strand. Copious PIE was observed with the same decay kinetics seen from identical samples fractured in the diffusion-pumped system. We therefore suspect strongly that the background gases in this system are not the source of the observed PIE. Further tests on BR will be carried out in the near future.

Thus, the current hypothesis in that the observed PIE originates from the constituents of the fracture surface. The monomer of polybutadiene has the structure:

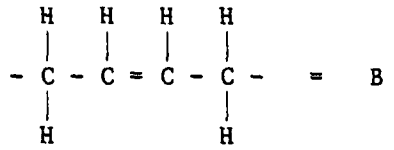

with molecular weight of 54. The final decomposition products of dicumyl peroxide are the relatively stable compounds acetophenone (M = 120 amu) and cumyl alcohol (M = 136 amu).[12] To determine if the peroxide products were necessary constituents for producing PIE from BR, we manufactured unfilled BR with no curing agent and cross-linked it with a) UV light from a Hg lamp, b) γ-rays from a Co^{60} source, and c) simply by heating the material in a press. All three methods yielded both EE and PIE, where a), b), and c) produced a decreasing order of emission intensities. Although we did not measure the PIE masses from these materials we believe we can safely conclude that the products of the curing agent are not responsible for the PIE we observe from BR.

It appears that the PIE indeed originates from the fractured material which involves the polymer and polymer-glass bead interface. Because oxygen is available during the cross-linking process, we cannot rule out oxidation products as possible constituents. Suggested fragments from BR alone and BR plus oxygen, with their corresponding M/q values in parentheses are shown in Table I, where we have assumed q = e. Our present resolution is such that additional H-atoms could easily be present to saturate the bonds available; also the mass peaks in Fig. 2 could well represent groups of unresolved masses differing by a few H-atoms.

The mass spectrum obtained by using this method implies that the PIE originates from fragments produced by fracture of the polymer. The relatively high value of $\bar{E}_o$ is believed due to the repulsion of the positive ions from the high concentration of surface charge produced by charge separation during

fracture. Such measurements may have considerable potential in probing details of the fracture process on an atomic and molecular level.

Additional experimental work on this particular technique in our laboratory will involve improving the vacuum environment to eliminate any role of background gases, improving the M/q resolution by use of ion optics and a longer drift tube, and investigating other materials.

We wish to thank Dr. A. N. Gent, University of Akron Institute of Polymer Science for providing us with the BR samples and thank both Dr. Gent and Dr. E. E. Donaldson, Washington State University, for helpful discussions.

This work was supported by the Office of Naval Research, Contract N0014-80-C-0213 and by a grant from the M. J. Murdock Charitable Trust.

References

1. J. T. Dickinson, P. F. Braunlich, L. Larson, and A. Marceau, Appl. Surf. Sci. 1, 515 (1978).

2. D. L. Doering, T. Oda, J. T. Dickinson, and P. F. Braunlich, Appl. Surf. Sci. 3, 196 (1979).

3. L. A. Larson, J. T. Dickinson, P. F. Braunlich, and D. B. Snyder, J. Vac. Sci. Technol. 16, 590 (1979).

4. J. T. Dickinson, D. B. Snyder, and E. E. Donaldson, J. Vac. Sci. Technol. 17, 429 (1980).

5. J. T. Dickinson, D. B. Snyder, and E. E. Donaldson, Thin Solid Films 72, 225 (1980).

6. J. T. Dickinson, E. E. Donaldson, and D. B. Snyder, J. Vac. Sci. Technol. 18, 238 (1981).

7. J. T. Dickinson, E. E. Donaldson, and M. K. Park, J. Mat. Sci. 16, 2897 (1981).

8. J. T. Dickinson and L. C. Jensen, J. Polymer Sci. Polymer Physics Ed., in press.

9. J. T. Dickinson, M. K. Park, E. E. Donaldson, and L. C. Jensen, J. Vac. Sci. Technol., 20, 436 (1982).

10. J. T. Dickinson, L. C. Jensen, and M. K. Park, J. Mat. Sci., in press.

11. J. T. Dickinson, L. C. Jensen, and M. K. Park, Appl. Phys. Lett., in press.

12. N. Ashikari, I. Kawashima, and T. Kawashima, Bull. Chem. Soc. Japan 40, 2597 (1967).

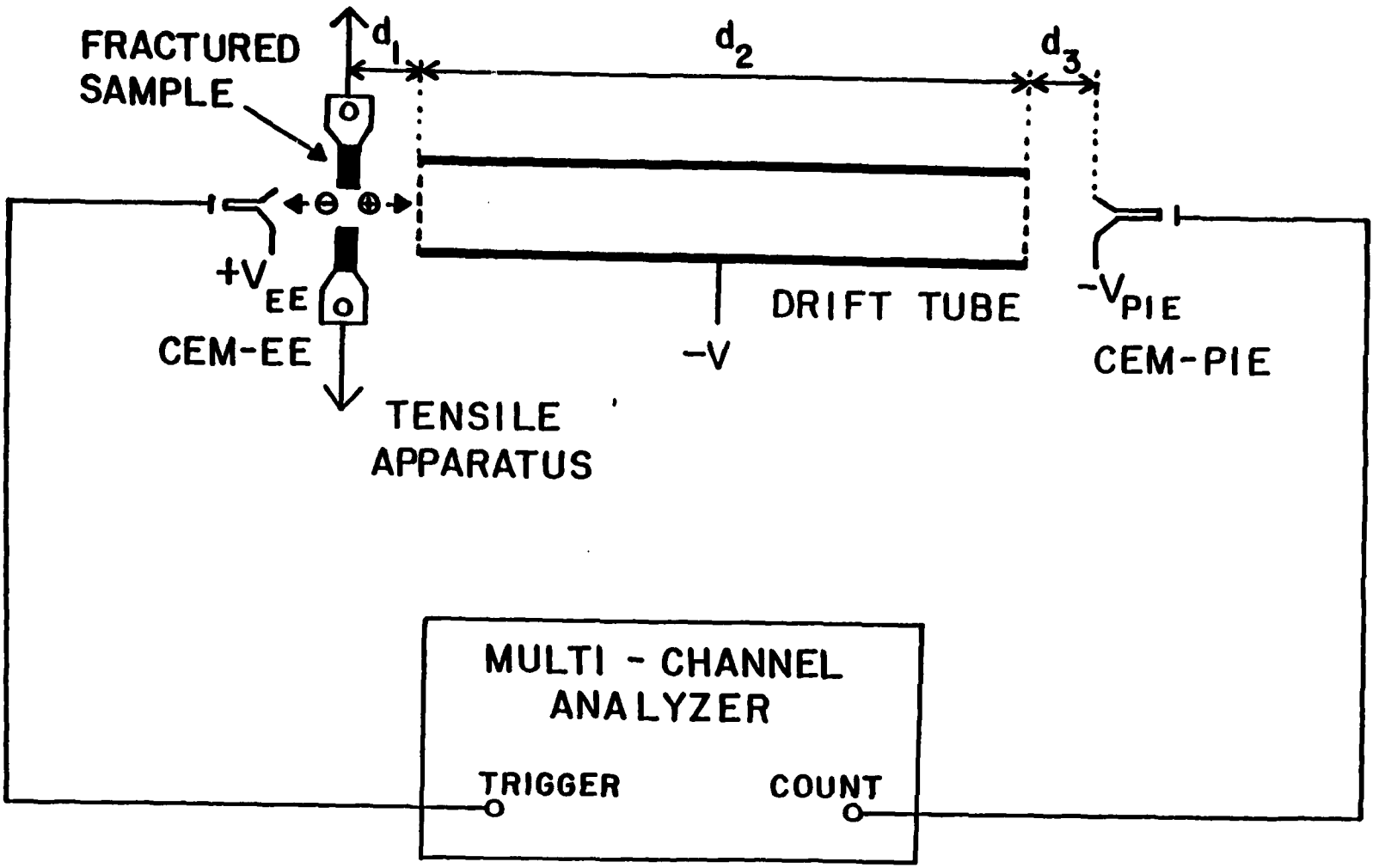

Fig. 1. Schematic diagram of time-of-flight apparatus for obtaining the M/q of positive ions released from a fractured sample.

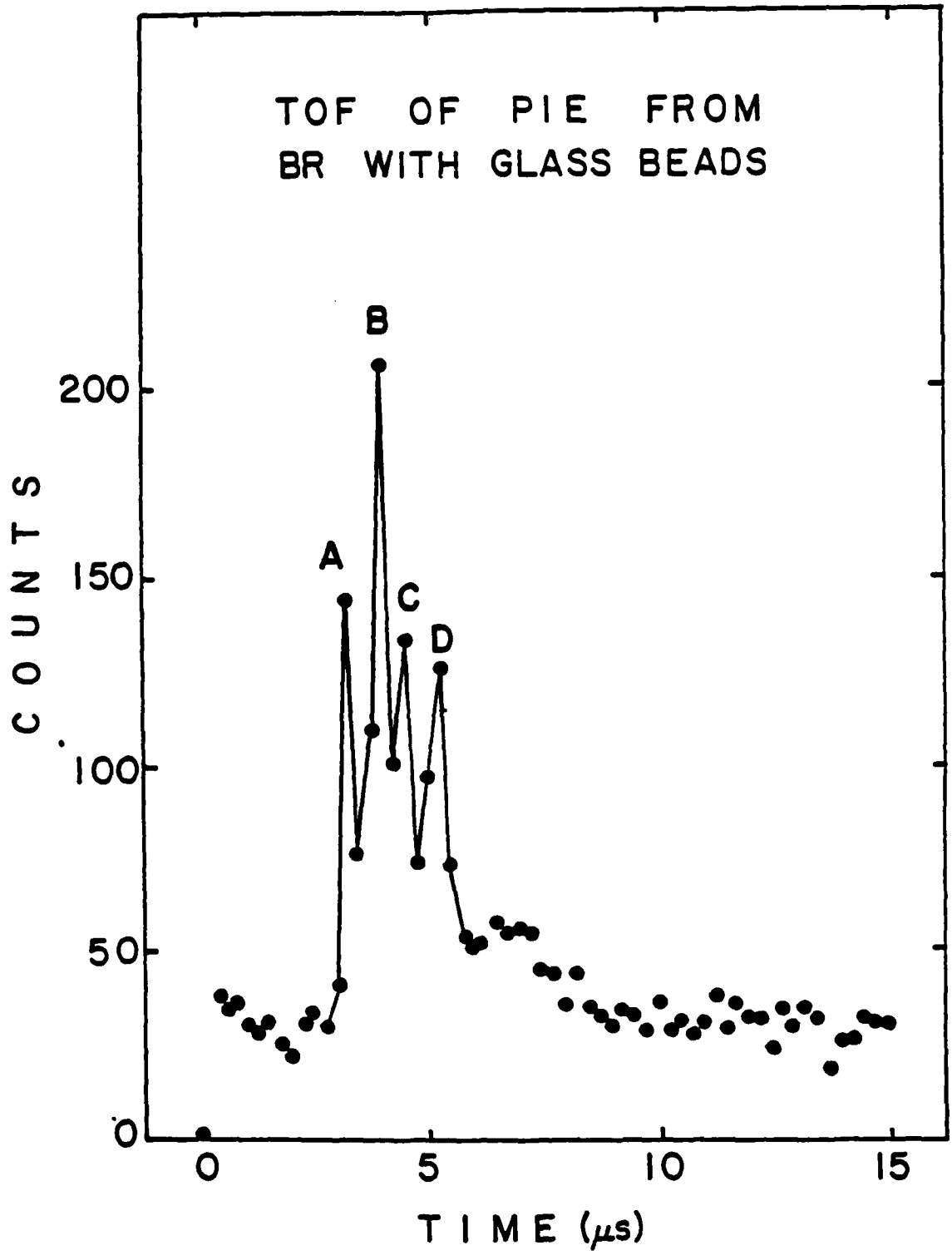

Fig. 2. Typical time-of-flight distribution for PIE from polybutadiene filled with glass beads. The drift-tube voltage was -2000V. Four major peaks labeled A, B, C, D are observed.

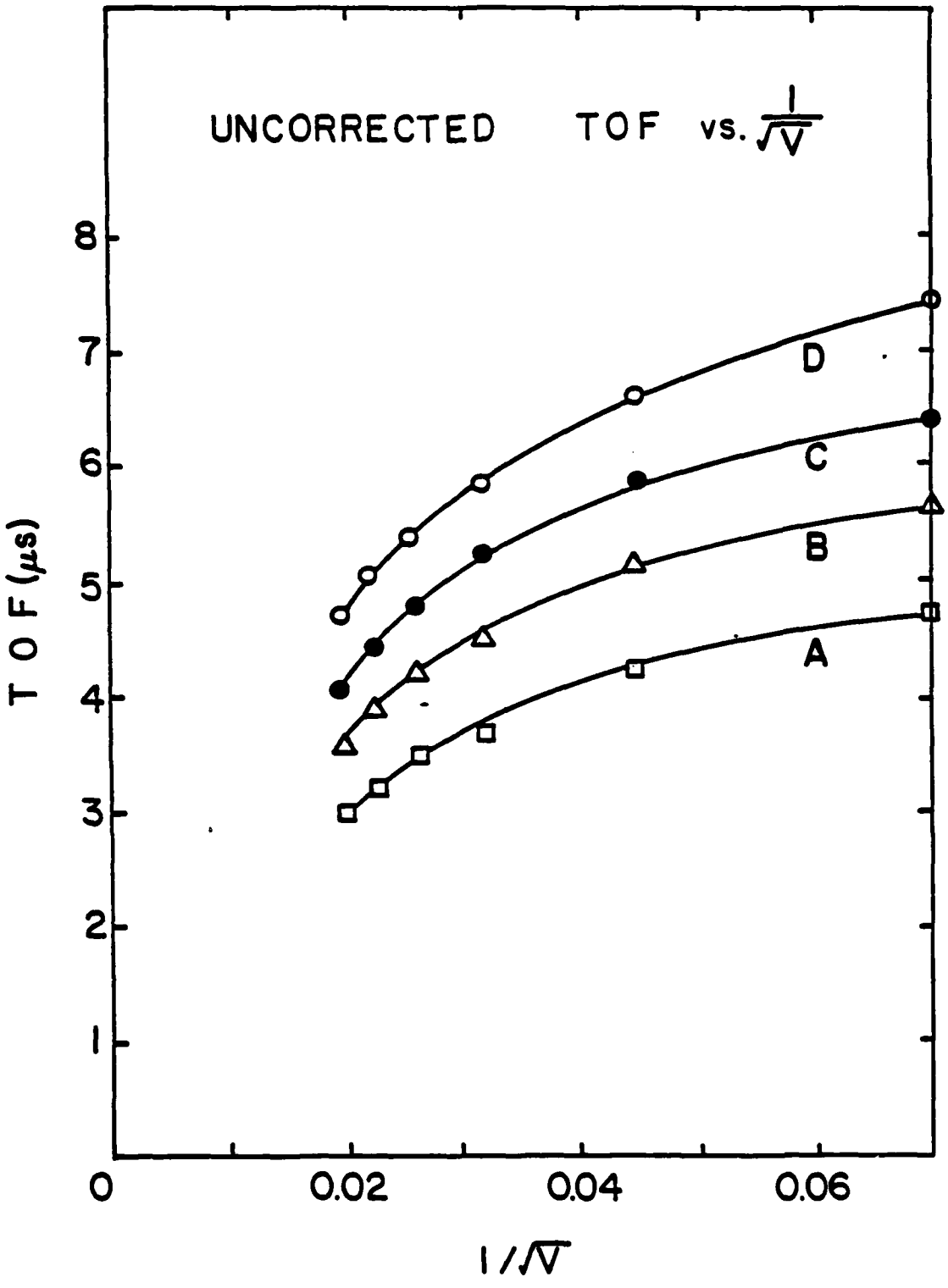

Fig. 3. The TOF vs $1/\sqrt{V}$ for the four peaks observed.

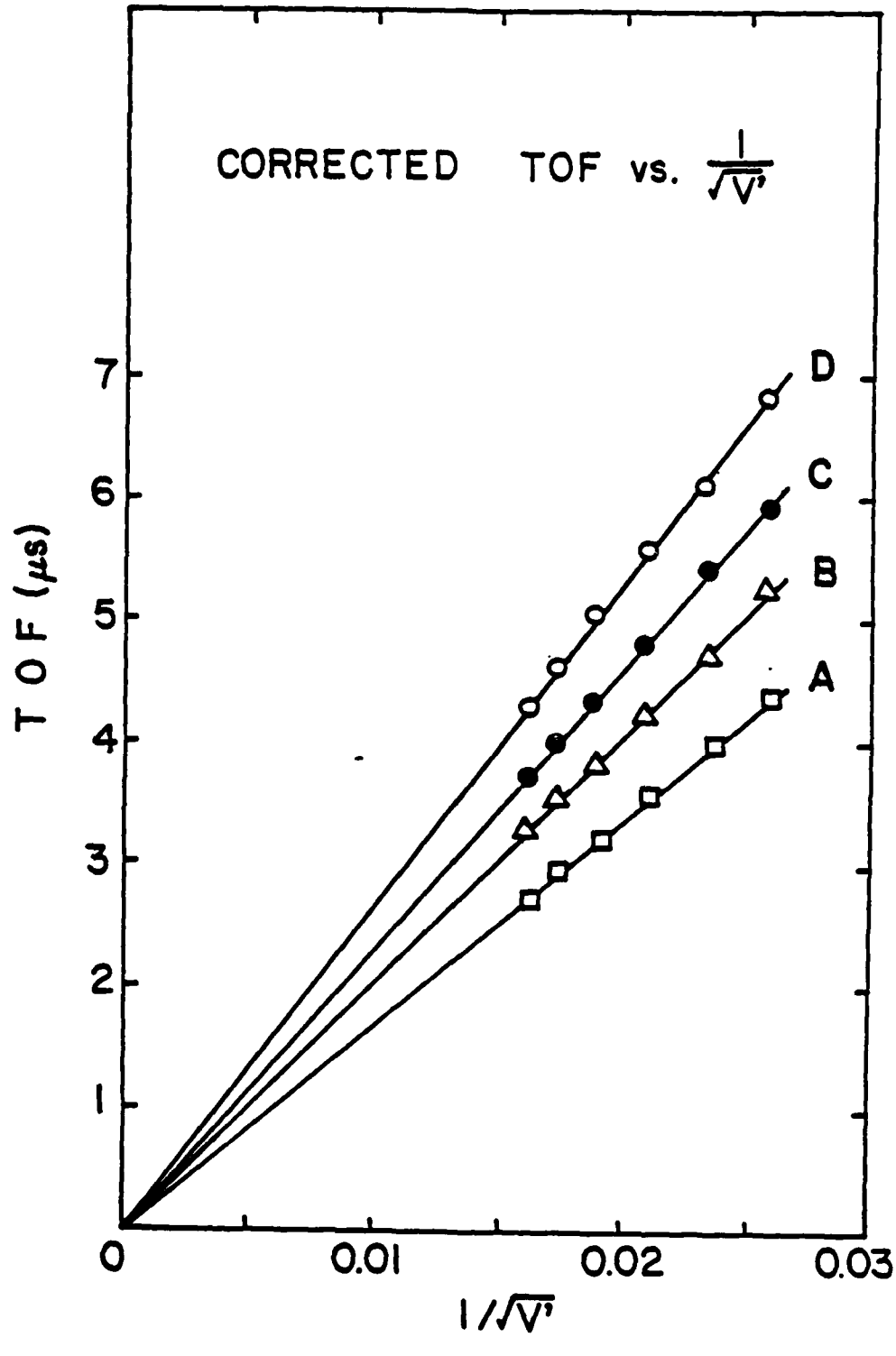

Fig. 4. The TOF vs $1/\sqrt{V'}$ where V' takes into account the PIE initial kinetic energy. The TOF has also been corrected slightly for the short times spent entering and leaving the drift tube.

VII. FRACTO-EMISSION FROM PENTAERYTHRITOL TETRANITRATE AND CYCLOTETRAMETHYLENE TETRANITRAMINE SINGLE CRYSTALS

M. H. Miles and J. T. Dickinson
Department of Physics
Washington State University
Pullman, WA 99164-2814

Abstract

Single crystals of pentaerythritol tetranitrate (PETN) and cyclotetramethylene tetranitramine (HMX) were fractured in vacuum while viewed by particle detectors strongly biased to separate positive and negative charge. Particles were detected on both detectors during and following fracture. Previous results on polymers suggest we are detecting electrons and positive ions. The observation of fracto-emission from these molecular crystals implies that crack propagation in such materials can break intramolecular bonds and the subsequent chemical reactions that lead to particle emission can continue for several minutes on the freshly created fracture surfaces.

INTRODUCTION

Recently the emission of electrons, positive ions, neutral particles, and photons have been observed from the fracture of many different types of solids.[1-12] In hard brittle solids, cracks can propagate with velocities as large as five to eight thousand meters per second and it appears clear that "mechanochemical" rupture of bonds occurs. What is not so evident is that intense particle emission and high electric fields can accompany the fracture event. Further, the emission observed frequently continues in a vacuum for a surprisingly long time after fracture, which we consider evidence for the high reactivity of fracture surfaces.

One solid type which to our knowledge has not been investigated for FE activity is the molecular solid or crystal. Here molecular units are held together by strong covalent bonds and the molecules are ordered into a crystal structure by weaker secondary bonds. The organic explosive solids pentaerythritol tetranitrate (PETN) and cyclotetramethylene tetranitramine (HMX) are of this molecular crystal type. Bowden[13] has reasoned that fracture would most likely separate molecules of the crystal rather than rupture bonds within the molecule. He thus concluded that it is unlikely that a "mechanochemical" mechanism would apply to simple organic explosives. However, Fox and Soria-Ruiz[14] fractured PETN and used a mass spectrometer to analyze the gaseous fragments produced. Their results indicated that the molecule cleaves at the four central C-C bonds producing fragments of the type CH_2-NO_3 and detectable amounts of NO_3-CH_2-C-CH_2-NO_3. They concluded that these fragments apparently decay towards CO and NO products.

Slow thermal decomposition of PETN produces many more products including NO_2, NO, N_2O, N_2, CO_2, CO, H_2, H_2O, and H_2CO.[15,16] This suggests that vibrational activated thermal bond breaking may be fundamentally different than stress dominated fracture bond rupture.

Various "mechanochemical" mechanisms as applied to exothermic materials have been proposed over the years.[17,18] The difficulty in obtaining experimental verification has prevented development of atomic understanding of these atomic reaction models. However, there has been recently a renewed interest in possible microscopic mechanisms by several groups of researchers.[19-22] The purpose of this communication is to present our first results on the emission of positive and negative charge during and following fracture of PETN and HMX. Our past experience with polymers[7,9,11,12] has shown that the negative charge emission consists principally of electrons and the positive charge emission consists of singly charged positive ions; we assume this to be the case with these materials also. We shall refer to the electron emission as EE and positive ion emission as PIE.

EXPERIMENTAL PROCEDURE

Small crystals (20 to 50 mg) of PETN and HMX were fractured in a vacuum chamber at a pressure of 10^{-7} torr. Charged particles were detected with two channel electron multipliers (CEM), Galileo Electro-Optics Model 4039, positioned on opposite sides of the sample at a distance of 1 cm. The front of the CEM was biased at +600 V for efficient detection of electrons and at -2500 V for detection of positive ions. Two detectors were used so that both negative and positive charge could be observed simultaneously. The pulse output (50 ns pulse width) of the CEMs were amplified and fed to 100 mHz discriminators whose outputs were counted by two multi-channel scalers (MCS) allowing counts versus time to be recorded for both EE and PIE.

Fracture of the small crystals was accomplished by placing them between two parallel metal surfaces in the vacuum system and closing the parallel surfaces by means of a bellows arrangement, crushing the crystals in

compression. Thus, the detectors were sampling only a thin layer of compressed material. On some occasions, after compression, the parallel metal surfaces were opened, increasing the effective area of surface sampled for emission. Compressive strain was chosen for these experiments because of the small size of the crystals and the difficulty one would have applying tensile forces to them. Failure in tension would tend to be better for FE studies because the crack tip and fracture surfaces would be in better communication with the vacuum. It should also be noted that the two detectors are viewing different fracture surfaces on opposite sides of the crushing mechanism, which may account for some of the minor differences we saw between the EE and PIE.

EXPERIMENTAL RESULTS

We fractured by compression five PETN crystals and three HMX crystals. Over time intervals of 80 to 100 seconds the fractured PETN crystals emitted detectable EE ranging from total counts of 100 to 85K and PIE ranging from 50 to 2K. MCS data accumulated at 0.2 seconds/channel for both EE and PIE are shown plotted on a log scale in Fig. 1a and 1b. Upon compression (started at the arrow marked C) we observed bursts of charged particle emission which decayed away in a few tenths of a second. In this particular data, the ions showed a decay which was non-exponential, similar to results for EE and PIE from polymer fracture and adhesive failure reported earlier.[7,9,11] Near the end of the run, the crushing surfaces were separated, which widened the gap to a few mm and exposed additional fracture surfaces to the vacuum. The time when the widening of this gap was started is shown by the arrow labeled O. Opening this gap generally caused an increase in emission. The erratic signal in Fig. 1 may be due to fragments of the crystal separating from other fragments. Fig. 2 shows the EE alone on a log scale for another PETN crystal

taken at 0.01 seconds/channel showing the rapid rise and relatively slow decay.

The emission from single crystal HMX was more intense and longer lasting than for PETN. Typical results for compressive fracture of HMX are shown in Fig. 3a and 3b. The metal surfaces compressing the crystal were separated a few mm at the arrow marked O, again causing an increase in emission. A clearer picture of the EE decay for HMX is shown in Fig. 4a at 0.8 seconds/channel. The first peak was generated by compression and the second peak occurred when the gap was opened a few mm. The emission is seen to last for several minutes. A third sample yielded the emission curve shown in Fig. 4b, where the tail of the decay is seen to be quite long lasting. The gap between the metal surfaces was opened and closed at the arrows marked O and C, respectively.

CONCLUSIONS

We have demonstrated charged particle emission accompanying and following fracture by compression of the molecular crystals PETN and HMX. Because the electric field produced by the front surfaces of the detectors is fairly high, the separation of plus and minus charges is likely for kinetic energies comparable to the energies we have observed in polymer fracture.[7-12] Thus we assume the detected particles from these molecular crystals are indeed of <u>both</u> negative and positive charge and consist of electrons and positive ions, although this needs to be confirmed. HMX showed more intense, longer lasting emission in comparison to PETN. Both materials showed emission decay curves similar to those observed from the fracture of polymers.

In the case of polymer fracture and adhesive failure, we have attributed the EE and PIE to surface chemical reactions of reactive species produced by

fracture. These reactions produce excited states that decay via non-radiative transitions into the observed charge states. The observation of EE and PIE from molecular crystals suggests that the fracture of these materials is accompanied by energetic bond scission which creates similar reactive species to those created in polymers.

We hope in future work to verify the tentative identification of electron and positive ion emission we have assigned to the FE from HMX and PETN reported here, to identify the mass of the PIE, and to measure the EE and PIE energy distributions. In polymers, the latter can be several hundred volts and is associated with the separation of charges. We have proposed that measurements of FE energy distributions may serve as a probe of the charge distributions produced on fracture surfaces of insulators.[7,9]

ACKNOWLEDGEMENTS

This work was supported by the Office of Naval Research under Contract N00014-80-C-0213.

We wish to thank Dr. Howard Cady, Los Alamos National Laboratory, for providing us with the single crystals of PETN and HMX. We also wish to thank Mr. Les Jensen and Mr. M. K. Park for their assistance in the laboratory.

References

1. J. T. Dickinson, P. F. Braunlich, L. Larson, and A. Marceau, Appl. Surf. Sci. 1, 515 (1978).
2. D. L. Doering, T. Oda, J. T. Dickinson, and P. F. Braunlich, Appl. Surf. Sci. 3, 196 (1979).
3. L. A. Larson, J. T. Dickinson, P. F. Braunlich, and D. B. Snyder, J. Vac. Sci. Technol. 16, 590 (1979).
4. J. T. Dickinson, D. B. Snyder, and E. E. Donaldson, J. Vac. Sci. Technol. 17, 429 (1980).
5. J. T. Dickinson, D. B. Snyder, and E. E. Donaldson, Thin Solid Films 72, 225 (1980).
6. J. T. Dickinson, E. E. Donaldson, and D. B. Snyder, J. Vac. Sci. Technol. 18, 238 (1981).
7. J. T. Dickinson, E. E. Donaldson, and M. K. Park, J. Mat. Sci. 16, 2897 (1981).
8. J. T. Dickinson and L. C. Jensen, J. Polymer Sci. Polymer Physics Ed., in press.
9. J. T. Dickinson, M. K. Park, E. E. Donaldson, and L. C. Jensen, J. Vac. Sci. Technol., 20 436 (1982).
10. J. T. Dickinson, L. C. Jensen, and M. K. Park, J. Mat. Sci., in press.
11. J. T. Dickinson, L. C. Jensen, and M. K. Park, Appl. Phys. Lett., in press.
12. J. T. Dickinson, L. C. Jensen, and M. K. Park, Appl. Phys. Lett., in press.
13. F. P. Bowden, "Proc. Ninth Int. Symp. Combustion," Academic Press, New York, 1963, p. 499.
14. P. G. Fox, J. Soria-Ruiz, Proc. R. Soc. A317, 79 (1970).
15. E. K. Rideal and A. J. B. Robertson, Proc. R. Soc. A195, 135 (1941).
16. J. Kimura and N. Kubota, Propellants Explos. 5, 1 (1980).

17. W. Taylor and A. Weale, Proc. Roy. Soc. A138, 92 (1932); Trans. Faraday Soc. 34, 995 (1938).

18. P. G. Fox, J. Solid State Chem. 2, 491 (1970).

19. F. J. Owens and J. Sharma, J. Appl. Phys. 51, 1494 (1980).

20. R. A. Graham, J. Phys. Chem. 83, 3048 (1979).

21. F. L. Walker, Propellants Explos. 7, 2 (1982).

22. M. Howard Miles, Doug Gustaveson, and K. L. DeVries, Bull. Am. Phys. Soc. 27, 198 (1982).

FRACTO-EMISSION FROM PETN

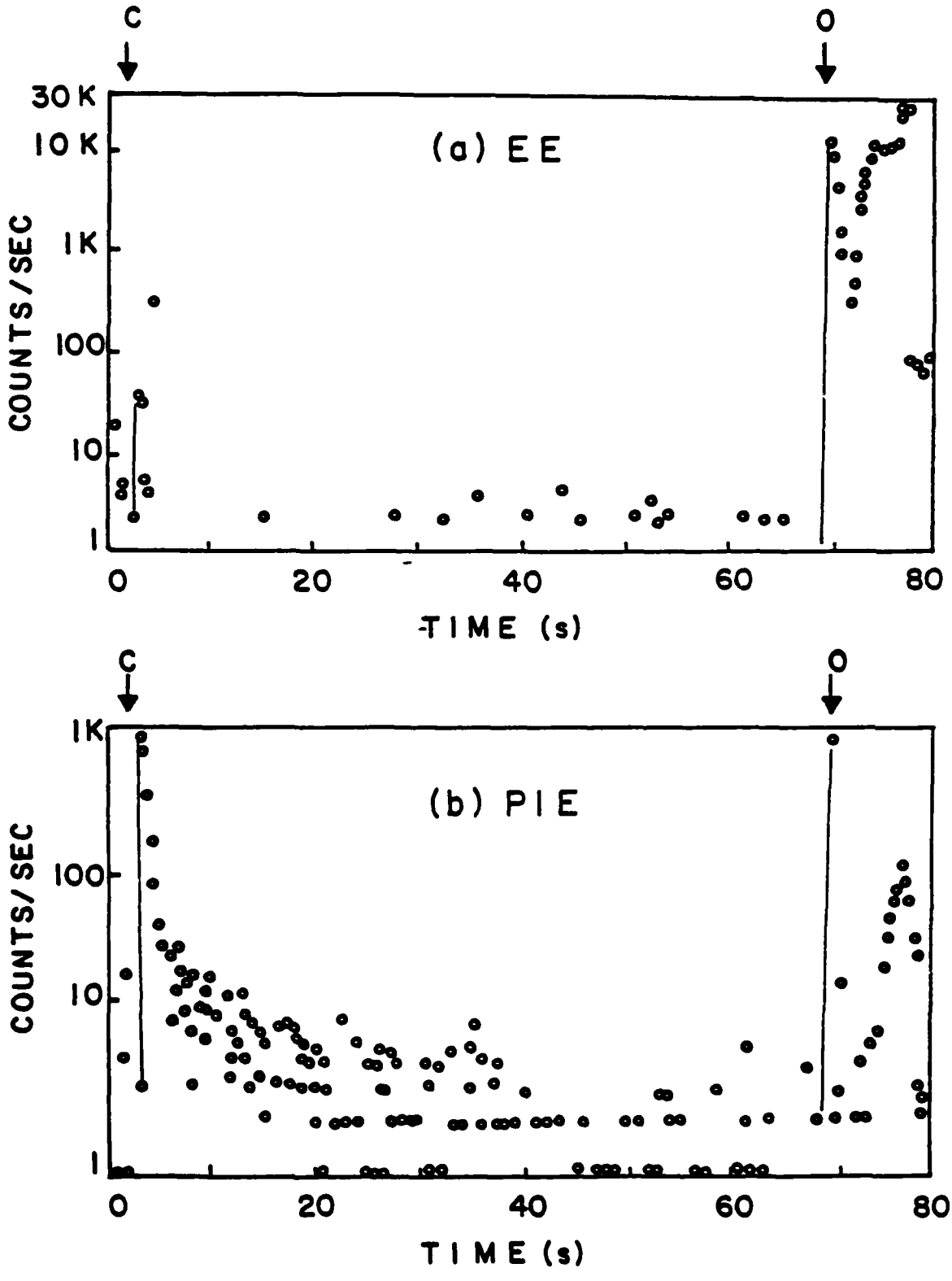

Fig. 1. The electron emission (a) and positive ion emission (b) accompanying and following fracture of a single crystal of PETN plotted on a log scale. C denotes the beginning of compression; O denotes opening of the crushing mechanism.

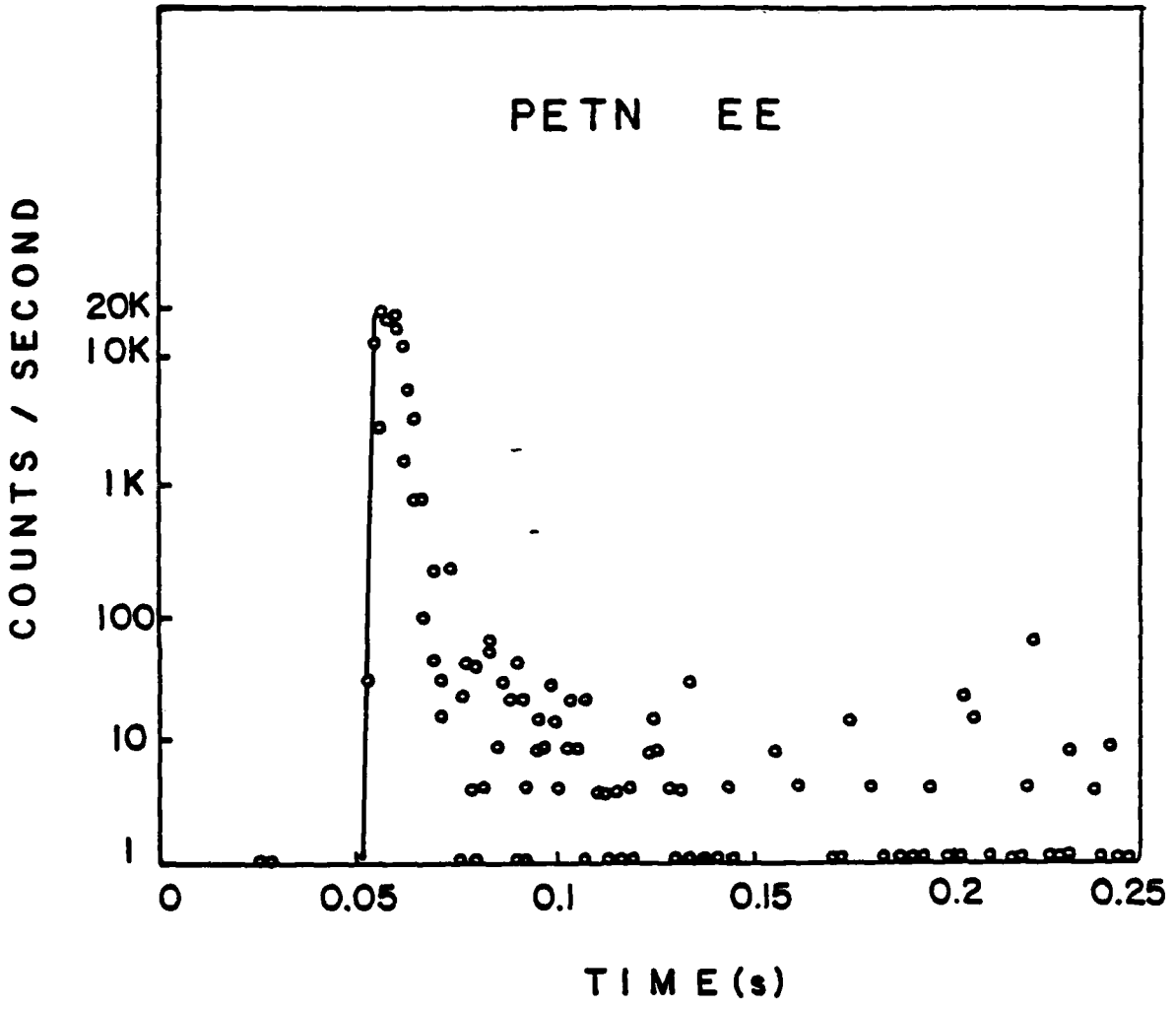

Fig. 2. Electron emission from fracture of a single crystal of PETN on a time scale of 0.01 seconds/channel. Count rate is plotted logarithmically.

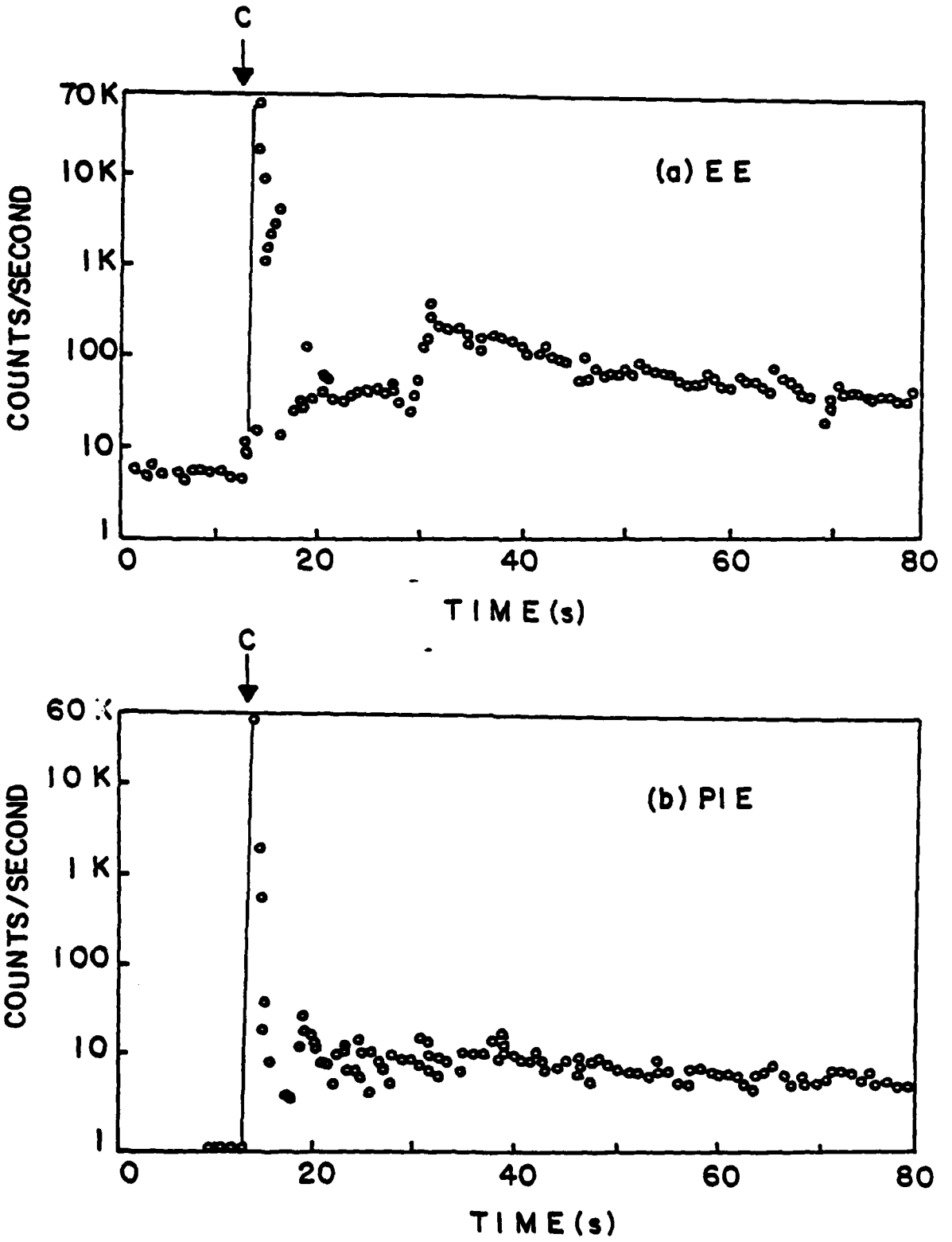

Fig. 3. Electron and positive ion emission from fracture of a single crystal of HMX on a log scale. Separation of the crushing mechanism is marked by O.

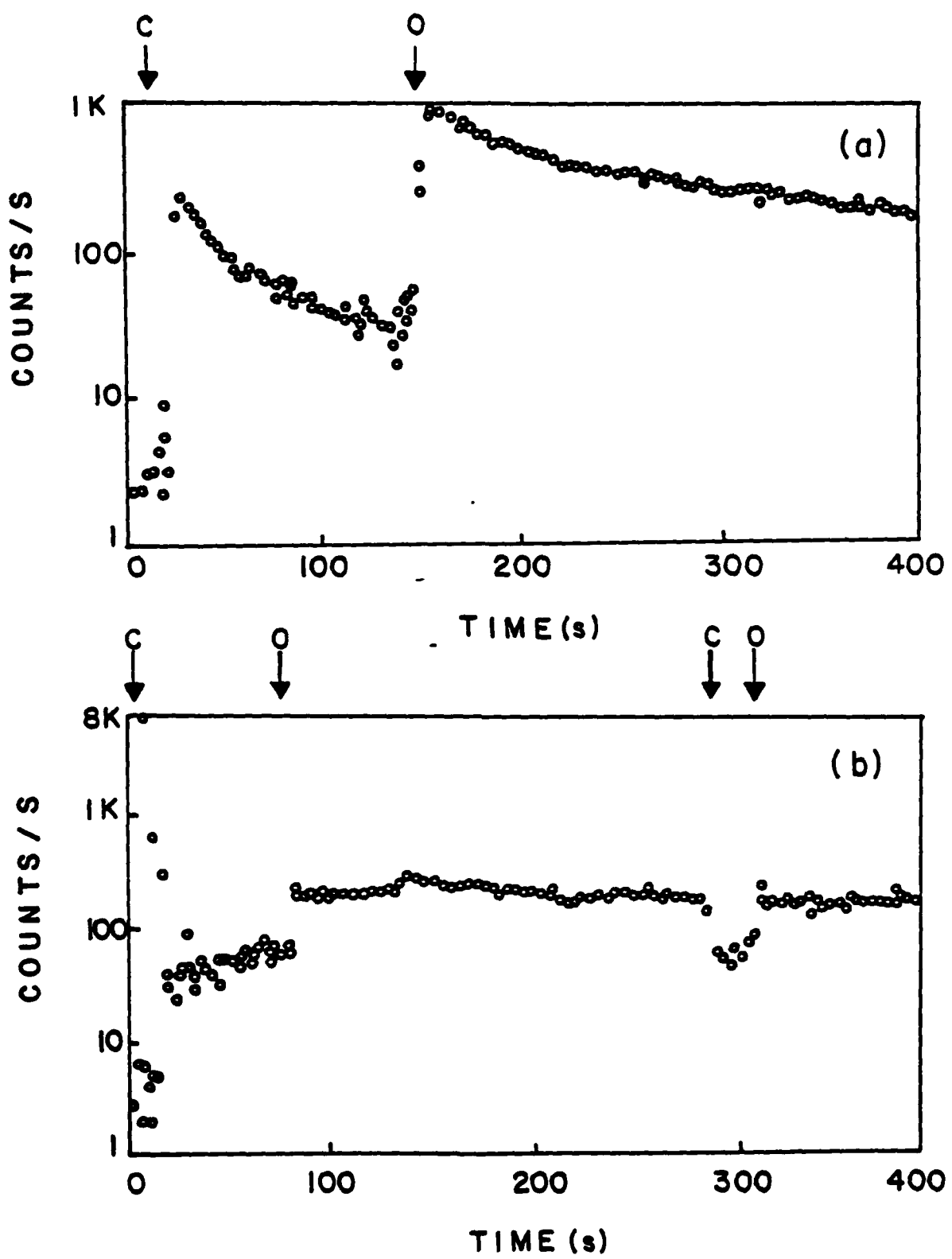

Fig. 4. Electron emission vs time for two HMX single crystals on a time scale of 0.8 seconds/channel. Crack closure is suspected to have stifled the decay of the EE in the first peak shown in (b).

VIII. CONCLUSION

The objectives of the work presented in this report were to characterize FE from the fracture of polymers, to further our understanding of FE mechanisms, and to relate the FE observed to the mechanical and chemical properties of the material undergoing fracture. Progress has been made in a number of areas by measurements involving interfacial failure, FE dependence on crack velocity, examining the time correlations between EE and PIE, development of TOF techniques to measure the M/q and kinetic energy of the PIE, and by measuring the EE and PIE from the fracture of molecular crystals .

Obviously, a great deal of effort is needed to further our understanding of the mechanisms of FE. As we make progress, however, a number of implications come into focus where potentially FE can play important roles. Briefly, we discuss these here.

First it is a probe of crack growth--it can serve as a measure of crack propagation on a sub-microsecond time scale. This could be of considerable utility in dynamic stress studies, e.g. on explosives, propellents, and in shock dynamics experiments. In addition, there is evidence that at relatively high strain rates electron emission can occur during the elongation of polymers without the occurrence of crack growth. This effect, reported by Zakrevskii and Pakhotin[1] is called mechano-emission. We are attempting to reproduce their results taking care to eliminate clamp slippage, microcracking on the edges of the polymer, and watching for craze formation during the elongation. Although our results are only preliminary, they support their observations. Thus FE may also be of use to dynamic loading experiments concerned with phenomena before the onset of crack growth.

Second, FE probes the electronic and chemical activity of the fracture surface. It indicates how rapidly and to what degree this activity builds up

and falls with fracture. Our results to date indicate that free radicals produced by fracture are playing a very important role in the production of FE.

The single particle counting capability we have for charged particles and photons appear to make our experiments extremely sensitive to the reactions of mechanically induced free radicals and/or other reactive species on the fracture surface. FE studies may be of considerable value to the study of fracture-induced chemistry such as observed by Goldanskii et al.[2] where they detected explosive phenomena in γ-irradiated chlorine-methyl cyclohexane upon fracture. As determined by Field et al.,[3] the fracture of a polymer, such as PS, in contact with PETN leads to ignition under impact at the polymer-explosive interface in the vicinity of the fracture. FE could in principle be used to monitor crack growth in the material on a sub-microsecond time scale while simultaneously measuring the onset of ignition. This would allow a better understanding of the connection between the two events.

Third, FE products generally strike the opposite crack wall. The intensity of FE we measure is several orders of magnitude smaller than what actually leaves the fracture surface due to collisions in the crack itself. Thus, if the fracture surface is chemically sensitive, possibly even activated due to the fracture, the bombardment of this surface with FE products may lead to important chemical processes.

Fourth, the energies of the charged FE observed is a probe of the charge density on the fracture surface and shows this density to be very high. At atmospheric pressure, this charge separation leads to electrical breakdown of the gases in the crack-tip. Much of the photon emission observed during fracture (tribo-luminescence) is attributed to break-down. Photon emission (phE) measurements can be made either in air, other gases, or vacuum. An understanding of the phE mechanisms could be gained by comparisons of emission curves in various gas environments. Since one would expect electrical break-

down in the crack tip to have considerable impact chemically on the freshly created crack walls, using FE as a means of studying this phenomenon could be an important application.

Fifth, there is considerable potential for the application of FE to the materials science aspects of fracture. In polymers, the FE may show where bonds are breaking, the FE being most intense when the degree of primary bond scission is high. It also is sensitive to the rate of bond breaking. FE may serve as a probe of the temperature of the fracture surface by the manner in which it affects the kinetics of FE decay. FE also has considerable potential as a probe of the locus of fracture in multi-component materials (e.g. adhesive vs. cohesive failure). It is, for example, possible to use FE to observe bead dewetting in a strained polymer filled with glass beads before fracture occurs.

Our future work will focus on the following topics:

a) The FE from energetic elastomers, filled and unfilled.

b) Determination of the role of background gases (if any).

c) Further V_c dependence measurements, at higher V_c.

d) Mass spectroscopy of the neutral emission.

e) Improved energy distribution measurements on EE and PIE.

f) Imaging energy distribution measurements on EE and PIE.

g) Examination of strain-rate effects, particularly where emission occurs prior to crack growth.

REFERENCES

1. V. A. Zakrevskii and V. A. Pakhotin, Sov. Phys. Solid State 20, 214 (1978).

2. A. M. Zanin, D. P. Kiryukhin, I. M. Barkhalov, and I. V. Gol-danskii, JETP Lett. 33, 321 (1981).

3. J. E. Field, M. M. Chaudhri, G. M. Swallowe, and T. B. Tang, Final Technical Report: Deformation and Thermal Properties of Energetic Materials, European Research Office, 1980.

IX. FRACTO-EMISSION TALKS AND PAPERS PRESENTED

"Fracto-Emission From Polymers" Naval Weapons Center (September 1981)

"Charged Particle Emission Accompanying Adhesive Failure" American Vacuum Society 28th National Symposium (November 1981)

"Fracto-Emission" 3M Center, St. Paul, Minnesota (November 1981)

"Electron, Positive Ion, and Photon Emission Accompanying and Following Fracture" American Physical Society Topical Conference on Deformation, Fracture, Wear, and NDE of Materials, New Orleans (November 1981)

"Particle Emission Accompanying Fracture" Department of Materials Science, Stanford University (January 1982)

"Fracto-Emission" McDonnell Douglas Research Laboratories (April 1982)

"Fracto-Emission" Los Alamos Scientific Laboratories (April 1982)

"Fracto-Emission" Sandia Laboratories (April 1982)

"Charge Particle Emission Accompanying Fracture of Materials" Pacific N.W. American Vacuum Society, Portland (May 1982)

DISTRIBUTION LIST

	No. Copies
Dr. L.V. Schmidt Assistant Secretary of the Navy (R,E, and S) Room 5E 731 Pentagon Washington, D.C. 20350	1
Dr. A.L. Slafkosky Scientific Advisor Commandant of the Marine Corps Code RD-1 Washington, D.C. 20380	1
Dr. Richard S. Miller Office of Naval Research Code 413 Arlington, VA 22217	10
Mr. David Siegel Office of Naval Research Code 260 Arlington, VA 22217	1
Dr. R.J. Marcus Office of Naval Research Western Office 1030 East Green Street Pasadena, CA 91106	1
Dr. Larry Peebles Office of Naval Research East Central Regional Office 666 Summer Street, Bldg. 114-D Boston, MA 02210	1
Dr. Phillip A. Miller Office of Naval Research San Francisco Area Office One Hallidie Plaza, Suite 601 San Francisco, CA 94102	1
Mr. Otto K. Heiney AFATL - DLDL Elgin AFB, FL 32542	1
Mr. R. Geisler ATTN: MKP/MS24 AFRPL Edwards AFB, CA 93523	1
Dr. F. Roberto Code AFRPL MKPA Edwards AFB, CA 93523	1
Dr. L.H. Caveny Air Force Office of Scientific Research Directorate of Aerospace Sciences Bolling Air Force Base Washington, D.C. 20332	1
Mr. Donald L. Ball Air Force Office of Scientific Research Directorate of Chemical Sciences Bolling Air Force Base Washington, D.C. 20332	1
Dr. John S. Wilkes, Jr. FJSRL/NC USAF Academy, CO 80840	1
Dr. R.L. Lou Aerojet Strategic Propulsion Co. P.O. Box 15699C Sacramento, CA 95813	1
Dr. V.J. Keenan Anal-Syn Lab Inc. P.O. Box 547 Paoli, PA 19301	1
Dr. Philip Howe Army Ballistic Research Labs ARRADCOM Code DRDAR-BLT Aberdeen Proving Ground, MD 21005	1
Mr. L.A. Watermeier Army Ballistic Research Labs ARRADCOM Code DRDAR-BLI Aberdeen Proving Ground, MD 21005	1
Dr. W.W. Wharton Attn: DRSMI-RKL Commander U.S. Army Missile Command Redstone Arsenal, AL 35898	1

DISTRIBUTION LIST

	No. Copies
Dr. R.G. Rhoades Commander Army Missile Command DRSMI-R Redstone Arsenal, AL 35898	1
Dr. W.D. Stephens Atlantic Research Corp. Pine Ridge Plant 7511 Wellington Rd. Gainesville, VA 22065	1
Dr. A.W. Barrows Ballistic Research Laboratory USA ARRADCOM DRDAR-BLP Aberdeen Proving Ground, MD 21005	1
Dr. C.M. Frey Chemical Systems Division P.O. Box 358 Sunnyvale, CA 94086	1
Professor F. Rodriguez Cornell University School of Chemical Engineering Olin Hall, Ithaca, N.Y. 14853	1
Defense Technical Information Center DTIC-DDA-2 Cameron Station Alexandria, VA 22314	12
Dr. Rocco C. Musso Hercules Aerospace Division Hercules Incorporated Alleghany Ballistic Lab P.O. Box 210 Washington, D.C. 21502	1
Dr. Ronald L. Simmons Hercules Inc. Eglin AFATL/DLDL Eglin AFB, FL 32542	1
Dr. E.H. Debutts Hercules Inc. Baccus Works P.O. Box 98 Magna, UT 84044	1
Dr. James H. Thacher Hercules Inc. Magna Baccus Works P.O. Box 98 Magna, UT 84044	1
Mr. Theordore M. Gilliland Johns Hopkins University APL Chemical Propulsion Info. Agency Johns Hopkins Road Laurel, MD 20810	1
Dr. R. McGuire Lawrence Livermore Laboratory University of California Code L-324 Livermore, CA 94550	1
Dr. Jack Linsk Lockheed Missiles & Space Co. P.O. Box 504 Code Org. 83-10, Bldg. 154 Sunnyvale, CA 94088	1
Dr. B.G. Craig Los Alamos National Lab P.O. Box 1663 NSP/DOD, MS-245 Los Alamos, NM 87545	1
Dr. R.L. Rabie WX-2, MS-952 Los Alamos National Lab. P.O. Box 1663 Los Alamos NM 37545	1
Dr. R. Rogers, WX-2 Los Alamos Scientific Lab. P.O. Box 1663 Los Alamos, NM 87545	1

DISTRIBUTION LIST

	No. Copies
Mr. R. Brown Naval Air Systems Command Code 330 Washington, D.C. 20361	1
Dr. H. Rosenwasser Naval Air Systems Command AIR-310C Washington, D.C. 20360	1
Mr. B. Sobers Naval Air Systems Command Code 03P25 Washington, D.C. 20360	1
Dr. L.R. Rothstein Assistant Director Naval Explosives Dev. Engineering Dept. Naval Weapons Station Yorktown, VA 23691	1
Dr. Lionel Dickinson Naval Explosive Ordnance Disposal Tech. Center Code D Indian Head, MD 20640	1
Mr. C.L. Adams Naval Ordnance Station Code PM4 Indian Head, MD 20640	1
Mr. S. Mitchell Naval Ordnance Station Code 5253 Indian Head, MD 20640	1
Dr. William Tolles Dean of Research Naval Postgraduate School Monterey, CA 93940	1
Naval Research Lab. Code 6100 Washington, D.C. 20375	1
Dr. J. Schnur Naval Research Lab. Code 6510 Washington, D.C. 20375	1
Mr. R. Beauregard Naval Sea Systems Command SEA 64E Washington, D.C. 20362	1
Mr. G. Edwards Naval Sea Systems Command Code 62R3 Washington, D.C. 20362	1
Mr. John Boyle Materials Branch Naval Ship Engineering Center Philadelphia, PA 19112	1
Dr. H.G. Adolph Naval Surface Weapons Center Code R11 White Oak Silver Spring, MD 20910	1
Dr. T.D. Austin Naval Surface Weapons Center Code R16 Indian Head, MD 20640	1
Dr. T. Hall Code R-11 Naval Surface Weapons Center White Oak Laboratory Silver Spring, MD 20910	1
Mr. G.L. Mackenzie Naval Surface Weapons Center Code R101 Indian Head, MD 20640	1
Dr. K.F. Mueller Naval Surface Weapons Center Code R11 White Oak Silver Spring, MD 20910	1

DISTRIBUTION LIST

	No. Copies
Mr. J. Murrin Naval Sea Systems Command Code 62R2 Washington, D.C. 20362	1
Dr. D.J. Pastine Naval Surface Weapons Cneter Code RC4 White Oak Silver Spring, MD 20910	1
Mr. L. Roslund Naval Surface Weapons Center Code R122 White Oak, Silver Spring MD 20910	1
Mr. M. Stosz Naval Surface Weapons Center Code R121 White Oak Silver Spring, MD 20910	1
Dr. E. Zimmet Naval Surface Weapons Center Code R13 White Oak Silver Spring, MD 20910	1
Dr. D. R. Derr Naval Weapons Center Code 388 China Lake, CA 93555	1
Mr. Lee N. Gilbert Naval Weapons Center Code 3205 China Lake, CA 93555	1
Dr. E. Martin Naval Weapons Center Code 3858 China Lake, CA 93555	1
Mr. R. McCarten Naval Weapons Center Code 3272 China Lake, CA 93555	1
Dr. A. Nielsen Naval Weapons Center Code 385 China Lake, CA 93555	1
Dr. R. Reed, Jr. Naval Weapons Center Code 388 China Lake, CA 93555	1
Dr. L. Smith Naval Weapons Center Code 3205 China Lake, CA 93555	1
Dr. B. Douda Naval Weapons Support Center Code 5042 Crane, Indiana 47522	1
Dr. A. Faulstich Chief of Naval Technology MAT Code 0716 Washington, D.C. 20360	1
LCDR J. Walker Chief of Naval Material Office of Naval Technology MAT, Code 0712 Washington, D.C. 20360	1
Mr. Joe McCartney Naval Ocean Systems Center San Diego, CA 92152	1
Dr. S. Yamamoto Marine Sciences Division Naval Ocean Systems Center San Diego, CA 91232	1
Dr. G. Bosmajian Applied Chemistry Division Naval Ship Research & Development Center Annapolis, MD 21401	1
Dr. H. Shuey Rohn and Haas Company Huntsville, Alabama 35801	1

DISTRIBUTION LIST

	No. Copies
Dr. J.F. Kincaid Strategic Systems Project Office Department of the Navy Room 901 Washington, D.C. 20376	1
Strategic Systems Project Office Propulsion Unit Code SP2731 Department of the Navy Washington, D.C. 20376	1
Mr. E.L. Throckmorton Strategic Systems Project Office Department of the Navy Room 1048 Washington, D.C. 20376	1
Dr. D.A. Flanigan Thiokol Huntsville Division Huntsville, Alabama 35807	1
Mr. G.F. Mangum Thiokol Corporation Huntsville Division Huntsville, Alabama 35807	1
Mr. E.S. Sutton Thiokol Corporation Elkton Division P.O. Box 241 Elkton, MD 21921	1
Dr. G. Thompson Thiokol Wasatch Division MS 240 P.O. Box 524 Brigham City, UT 84302	1
Dr. T.F. Davidson Technical Director Thiokol Corporation Government Systems Group P.O. Box 0263 Ogden, Utah 84409	1
Dr. C.M. Vriesen Thiokol Elkton Division P.O. Box 241 Elkton, MD 21921	1
Dr. J.C. Hinshaw Thiokol Wasatch Division P.O. Box 524 Brigham City, Utah 84302	1
U.S. Army Research Office Chemical & Biological Scier Division P.O. Box 12211 Research Triangle Park NC 27709	1
Dr. R.F. Walker USA ARRADCOM DRDAR-LCE Dover, NJ 07801	1
Dr. T. Sinden Munitions Directorate Propellants and Explosives Defence Equipment Staff British Embassy 3100 Massachusetts Ave. Washington, D.C. 20008	1
LTC B. Loving AFROL/LK Edwards AFB, CA 93523	1
Professor Alan N. Gent Institute of Polymer Science University of Akron Akron, OH 44325	1
Mr. J. M. Frankle Army Ballistic Research Labs ARRADCOM Code DRDAR-BLI Aberdeen Proving Ground, MD 21005	1

DISTRIBUTION LIST

	No. Copies
Dr. Ingo W. May Army Ballistic Research Labs ARRADCOM Code DRDAR-BLI Aberdeen Proving Ground, MD 21005	1
Professor N.W. Tschoegl California Institute of Tech Dept. of Chemical Engineering Pasadena, CA 91125	1
Professor M.D. Nicol University of California Dept. of Chemistry 405 Hilgard Avenue Los Angeles, CA 90024	1
Professor A. G. Evans University of California Berkeley, CA 94720	1
Professor T. Litovitz Catholic Univ. of America Physics Department 520 Michigan Ave., N.E. Washington, D.C. 20017	1
Professor W. G. Knauss Graduate Aeronautical Lab California Institute of Tech. Pasadena, CA 91125	1
Professor Edward Price Georgia Institute of Tech. School of Aerospace Engin. Atlanta, Georgia 30332	1
Dr. Kenneth O. Hartman Hercules Aerospace Division Hercules Incorporated P.O. Box 210 Cumberland, MD 21502	1
Dr. Thor L. Smith IBM Research Lab D42.282 San Jose, CA 95193	1
Dr. J. P. Marshall Dept. 52-35, Bldg. 204/2 Lockheed Missile & Space Co. 3251 Hanover Street Palo Alto, CA 94304	1
Ms. Joan L. Janney Los Alamos National Lab Mail Stop 920 Los Alamos, NM 87545	1
Dr. J. M. Walsh Los Alamos Scientific Lab Los Alamos, NM 87545	1
Professor R. W. Armstrong Univ. of Maryland Department of Mechanical Eng. College Park, MD 20742	1
Prof. Richard A. Reinhardt Naval Postgraduate School Physics & Chemistry Dept. Monterey, CA 93940	1
Dr. R. Bernecker Naval Surface Weapons Center Code R13 White Oak, Silver Spring, MD 20910	1
Dr. M. J. Kamlet Naval Surface Weapons Center Code R11 White Oak, Silver Spring, MD 20910	1
Professor J. D. Achenbach Northwestern University Dept. of Civil Engineering Evanston, IL 60201	1
Dr. N. L. Basdekas Office of Naval Research Mechanics Program, Code 432 Arlington, VA 22217	1
Professor Kenneth Kuo Pennsylvania State Univ. Dept. of Mechanical Engineering University Park, PA 16802	1

DISTRIBUTION LIST

	No. Copies	No. Copies
Dr. S. Sheffield Sandia Laboratories Division 2513 P.O. Box 5800 Albuquerque, NM 87185	1	
Dr. M. Farber Space Sciences, Inc. 135 Maple Avenue Monrovia, CA 91016	1	
Dr. Y. M. Gupta SRI International 333 Ravenswood AVenue Menlo Park, CA 94025	1	
Mr. M. Hill SRI International 333 Ravenswood Avenue Menlo Park, CA 94025	1	
Professor Richard A. Schapery Texas A&M Univ. Dept of Civil Engineering College Station, TX 77843	1	
Dr. Stephen Swanson Univ. of Utah Dept. of Mech. & Industrial Engineering MEB 3008 Salt Lake City, UT 84112	1	
Mr. J. D. Byrd Thiokol Corp. Huntsville Huntsville Div. Huntsville, AL 35807	1	
Professor G. D. Duvall Washington State University Dept. of Physics Pullman, WA 99163	1	
Prof. T. Dickinson Washington State University Dept. of Physics Pullman, WA 99163	1	